Chemical Investigation on the Mechanism and Kinetics of the Atmospheric Degradation Reaction of Trichlorofluoroethene by $OH^{\bullet}$ and Its Subsequent Fate in the Presence of O_2/NOx

Abolfazl Shiroudi,*[a,b] Jacek Czub,[a,b] and Mohammednoor Altarawneh[c]

[a] *Department of Physical Chemistry, Gdańsk University of Technology, Narutowicza 11/12, Gdańsk 80-233, Poland*

[b] *BioTechMed Center, Gdańsk University of Technology, Gdańsk 80-233, Poland*

[c] *United Arab Emirates University, Department of Chemical and Petroleum Engineering, Sheikh Khalifa bin Zayed Street, Al-Ain 15551, United Arab Emirates*

Abstract

The M06-2X/6-311++G(d,p) level of theory was used to examine the degradation of Trichlorofluoroethene (TCFE) initiated by $OH^{\bullet}$ radicals. Additionally, the coupled-cluster single-double with triple perturbative [CCSD(T)] method was employed to refine the single-point energies using the complete basis set extrapolation approach. The results indicated that OH-addition is the dominant pathway. $OH^{\bullet}$ adds to both the C1 and C2 carbons, resulting in the formation of the $C(OH)Cl_2–{}^{\bullet}CClF$ and ${}^{\bullet}CCl_2–C(OH)ClF$ species. The associated barrier heights were determined to be 1.11 and –0.99 kcal mol^{-1}, respectively. Furthermore, the energetic and thermodynamic parameters show that pathway **1** exhibits greater exothermicity and exergonicity compared to pathway **2**, with differences of 8.11 and 8.21 kcal mol^{-1}, correspondingly. The primary pathway involves OH addition to the C2 position, with a rate constant of 6.2×10^{-13} cm^3 $molecule^{-1}$ sec^{-1} at 298 K. This analysis served to estimate the atmospheric lifetime, along with the photochemical ozone creation potential (POCP) and ozone depletion potential (ODP). It yielded an atmospheric lifetime of 8.49 days, an ODP of 4.8×10^{-4}, and a POCP value of 2.99, respectively. Radiative forcing efficiencies were also estimated at the M06-2X/6-311++G(d,p) level. Global warming potentials (GWPs) were calculated for 20, 100, and 500 years, resulting in values of 9.61, 2.61, and 0.74, respectively. TCFE is not expected to make a significant contribution to the radiative forcing of climate change. The results obtained from the time-dependent density functional theory (TDDFT) indicated that TCFE and its energized adducts are unable to photolysis under sunlight in the UV and visible spectrum.

* Corresponding author:
E-mail: abolfazl.shiroudi@pg.edu.pl (A. Shiroudi)

Secondary reactions involve the [TCFE-OH–O_2]$^{\bullet}$ peroxy radical, leading subsequently to the [TCFE-OH–O]$^{\bullet}$ alkoxy radical. It was found that the alkoxy radical resulting from the peroxy radical can lead to the formation of phosgene ($COCl_2$) and carbonyl chloride fluoride (CClFO), with phosgene being the primary product.

Introduction

Chlorofluorocarbons (CFCs), which possess special characteristics like low flammability, good chemical stability, reasonable cost, and low toxicity, are extensively employed in households and industries.[1] Chlorofluorocarbons are typically released into the atmosphere during different stages of their usage, mostly near the Earth's surface. Due to their stability, CFCs experience minimal losses in the troposphere and are predominantly eliminated in the stratosphere through short-wavelength UV photodissociation ($\lambda < 220$ nm), with some additional elimination occurring via gas-phase reactions with O(^{1}D). The decay time of CFCs in the atmosphere is influenced by a mixture of photochemical reactions, the reduction that occurs through the O(^{1}D) reaction, and the duration it takes for the air to move into and out of the stratosphere, resulting in $t_{1/2} > \sim 50$ years.[2]

The significance of CFCs in stratospheric ozone chemistry lies in their ability to serve as a reactive chlorine source and participate in catalytic ozone destruction cycles. Therefore, the loss mechanisms that occur in the atmosphere and the duration for which CFC-11 (CCl_3F) persists are particularly important, as this compound serves as the standard reference in calculating ozone depletion potentials (ODPs).[2] CFCs' chemical stability is critical in facilitating their gradual transport from the troposphere to the stratosphere.[3] Thus, it is important to comprehend the atmospheric chemistry and environmental impact of CFC alternatives to minimize their negative effects. Determining the atmospheric lifetime of a compound can help in predicting the intensity of any harmful effects.[4] Compounds with C=C bonds are highly reactive in the troposphere and degrade faster than CFCs.[5]

Trichloroethene (TCE) is a solvent commonly used by industry and is frequently found in contaminated groundwater.[6] It is considered a possible carcinogen for humans.[7] Injecting TCE into the groundwater as it passes through treatment layers is an alternate technique for treating contaminated water. Although chlorofluoroethenes (CFEs), including trichlorofluoroethene (TCFE), are not commonly used in industry.[8] Laboratory studies have shown that under anaerobic conditions, TCE and TCFE undergo similar reductive dechlorination reactions to form less chlorinated products.[9] The rates at which TCFE

undergoes reductive dechlorination are similar to that of perchloroethene and TCE. Also, TCFE and TCE follow second-order kinetics during reductive dechlorination, and the transformation rates of TCFE in the groundwater at specific chemical manufacturing plants are significantly higher than those of TCE.[9]

The concentration of TCE in groundwater can vary from very low levels, often measured in parts per billion (ppb), to concentrations as high as parts per million (ppm). The specific concentration depends on the source and extent of contamination. In unpolluted surface waters, like oceans, TCE concentrations typically range from 0.0001 to 0.02 µg/lit. In other areas, concentrations may vary from < 0.0001 to ~10 µg/lit, but the majority of measurements remain at 1 µg/lit or lower. Groundwater levels are subject to variation and local contamination, with concentrations usually falling within the range of 0.2 to 2 µg/lit. However, groundwater measurements have revealed much higher levels in areas with known contamination, with recorded levels reaching as high as 950 mg/lit. In drinking water, TCE levels are generally below 1 µg/lit, although some reports have cited higher levels, reaching up to 49 µg/lit.[10] Furthermore, TCE concentrations in the atmosphere can vary from negligible levels to exceeding regulatory standards, particularly in regions with extensive industrial activity or known contamination. In industrial areas, atmospheric TCE levels can fall within the ppb range and, in certain conditions, ppm. Within the atmosphere, TCE can undergo reactions with OH radicals produced through photochemical processes, leading to the formation of compounds like phosgene, dichloroacetyl chloride, formyl chloride, and other degradation products. Reported half-lives for the reaction with OH radicals range from 1 day to 2.5 weeks, with the potential for even longer half- lives, extending to several months during winter in polar regions.[11]

Halogenated alkenes, characterized by a strong infrared absorption due to the C–F bond, may have a role in global warming despite their presence in low quantities.[12] In addition, the ozone layer can be damaged by chlorinated compounds that release chlorine into the atmosphere. The objective of this work is to investigate the mechanism, thermochemistry, and reaction kinetics involved in the degradation of Trichlorofluoroethene (CFC-1111) as chlorofluorocarbons by OH radicals.

The atmospheric implications of TCFE were explored, including (*i*) evaluating various aspects such as reaction channels, branching ratios, atmospheric lifetime, photochemical ozone creation potential (POCP), and ozone depletion potential (ODP). These assessments were carried out by examining the rate constants of reactions between TCFE and OH radicals over the temperature ranging from 250 to 450 K, and (*ii*) Furthermore, the study also assessed

the radiative forcing efficiency (RFE) and the global warming potential (GWP) associated with TCFE. Therefore, understanding the degradation of TCFE into its end-products and assessing the potential consequences of these degradation products on other environmental concerns has become critical.

To the best of our knowledge, comprehensive theoretical research on the degradation of TCFE initiated by $OH^{\bullet}$ radicals has not been conducted. Our initial objective is to identify all feasible pathways and subsequently analyze the thermodynamics and kinetics of each reaction channel involved. This approach will enable us to gain a more comprehensive understanding of the degradation process. Density functional theory (DFT)[13] is a reliable and powerful tool for investigating thermochemistry and kinetics. Our analysis will cover the kinetics and thermochemistry of all pathways within the temperature range of 250 to 450 K, using transition state theory (TST)[14] in conjunction with the M06-2X functional and the 6-311++G(d,p) basis set,[15] as well as coupled-cluster theory [CCSD(T)],[16] to provide us with the thermodynamics and kinetics of this reaction. Additionally, we will explore the photodegradation mechanisms of TCFE in the gas phase using the time-dependent density functional theory (TDDFT) method.[17]

Results and Discussion

The degradation reactions between TCFE and hydroxyl radicals involve two reaction types: The first pathway involves the attack of $OH^{\bullet}$ onto the C1 and C2 positions; the second pathway involves the abstraction of a chlorine atom bonded to the C1 and C2 atoms. This specifically occurs through chlorine abstraction from the C1–Cl3, C1–Cl4, and C2–Cl6 bonds. The pre-reactive complex (pre-RC) is a frequent characteristic of reactions involving radical species and unsaturated molecules.[18] This pre-RC arises due to long-range Coulomb interactions between the isolated reactants.[19]

OH Radical-Initiated Reaction

Properties of the Stationary Points' Structure

Because of the presence of an unsaturated C–C bond, TCFE reacts with hydroxyl radicals via two pathways: (*i*) abstraction of the Cl-atom from the C–Cl bond; and (*ii*) $OH^{\bullet}$ addition to the C=C bond. When the $OH^{\bullet}$ radicals are added to the C1 position of the double bond, $C(OH)Cl_2–{}^{\bullet}CClF$ energetic adducts are formed while adding it to the C2 carbon leads to the

production of the $^{\bullet}CCl_2$–C(OH)FCl species. Similarly, abstraction of either chlorine gives rise to the HOCl and $^{\bullet}$CCl=CFCl or $Cl_2C=^{\bullet}CF$ radicals. Hence, it is expected that this reaction will involve these five reaction channels, as shown in Scheme 1. It is worth noting that the two chlorine atoms bonded to the C1 atom in TCFE are not identical, as depicted in Fig. 1. The (*Z*)-C–Cl bond is 0.004 Å shorter than the (*E*)-C–Cl bond. Hence, the (*E*)-chlorine atom is more likely to be abstracted faster by hydroxyl radicals than the (*Z*)-chlorine atom. However, it is believed that all five pathways initiate via the production of pre-reactive complexes denoted as pre-RC*n* (*n* =1–5).

Table 1 enlists the energies and thermodynamic parameters of the optimized stationary points involved in the degradation of TCFE initiated by hydroxyl radicals along five reactions **1**–**5**, which are labeled based on the atom labels given in Scheme 1. These calculations were performed using the M06-2X/6-311++G(d,p) level and were necessary for studying the overall reaction kinetics. The Cartesian coordinates and energetic and thermodynamic parameters of all species can be found in Table S1 of the Supporting Information. It is worth mentioning that all studied channels follow an indirect pathway via the formation of pre-RC species at the entry pathway.

There are two possible reactions for the addition of OH radicals to the double bond. The first reaction, referred to as **R1**, involves the addition of hydroxyl radicals at the C2 position via the formation of a **pre-RC1** species. In the **pre-RC1** species, the oxygen of the hydroxyl group is weakly bonded to the double bond at the C–F site, with a bond length of 2.645 Å. This reaction produces energized adducts, IM2, by forming the TS1 structure. In the TS1 species, the bond length between the OH radical and the C2 atom changes from 2.13 to 1.35 Å in the IM2 species. The second channel, denoted as **R2**, involves hydroxyl radicals attacking the C1 position via the formation of **pre-RC2** species. In this pre-reactive complex, the oxygen atom of the hydroxyl radicals is also weakly bonded to the double bond, with a bond length of 2.567 Å. The **R2** reaction pathway leads to the formation of intermediate radicals, IM6, via the formation of the TS6 species. In the TS6, the bond distance between the OH radical approaching the central carbon changes from 2.07 to 1.35 Å in the energized adducts IM6.

According to Hammond's postulate,[20] the consistent transition state (TS1/TS6) appears to be much more similar to the related pre-RC complexes (pre-RC1/RC2) for both pathways than to the energized adducts (IM2/IM6). The formation of the C1–O bond is smaller by

~0.06 Å in the TS6 species for reaction **2** than in the TS1 species for reaction **1** (see Figure S1, Supporting Information).

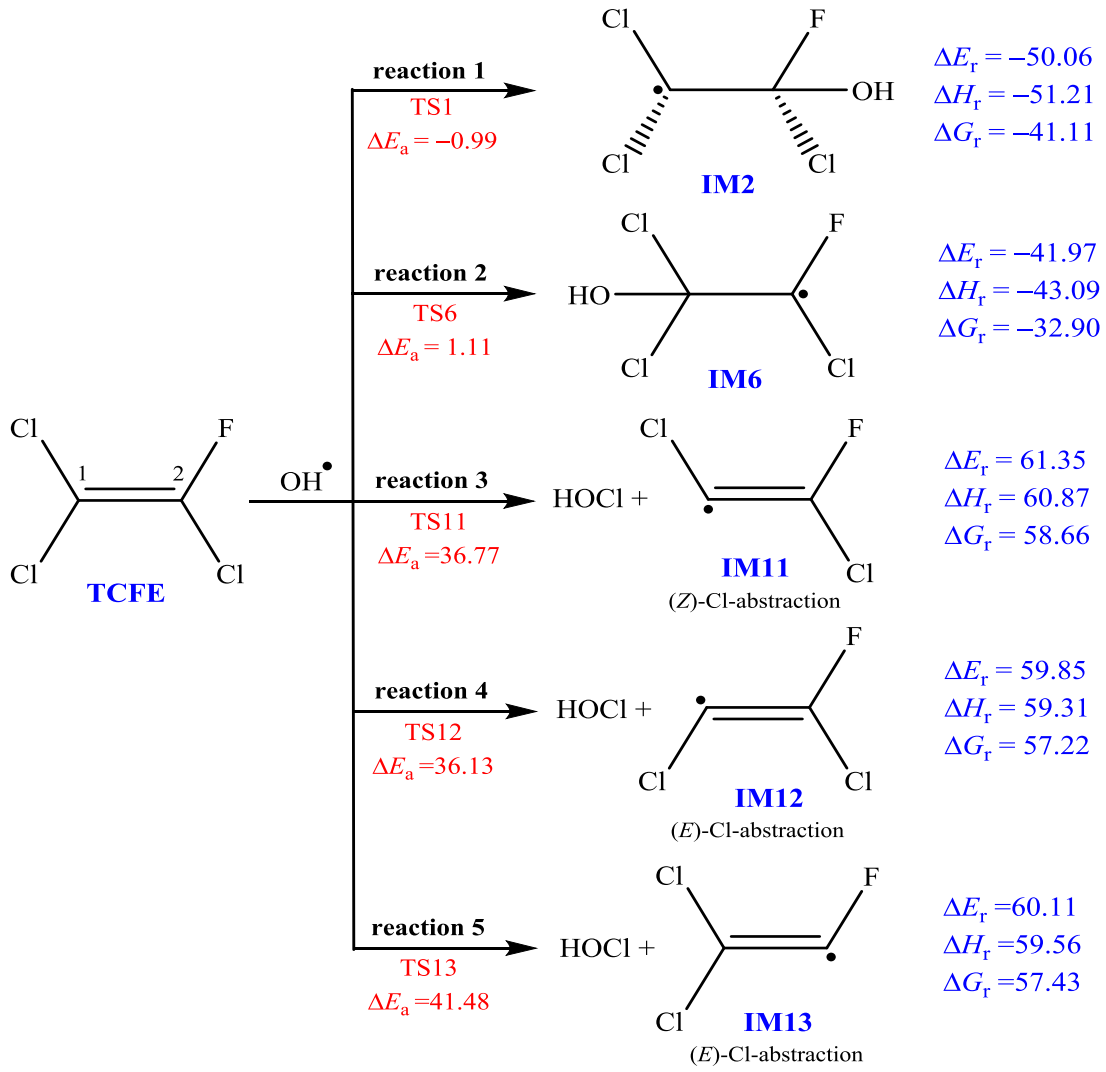

Scheme 1. Different channels involved in the atmospheric degradation mechanism of TCFE initiated by OH radicals (All reaction energy and energy barrier calculated at the M06-2X/6-311++G(d,p) level of theory are given in kcal mol^{-1})

Because the C–Cl bond is longer than the C–F bond and the chlorine atom is positioned farther from the nucleus, there is a higher tendency for the abstraction of the chlorine compared to the fluorine. As a result, our investigation will exclusively focus on elimination reactions involving the removal of three chlorine atoms. The abstraction reaction between TCFE and OH• radicals has three different pathways, with each pathway involving the abstraction of different chlorine. In pathway **3** (**R3**), the (*Z*)-chlorine atom is abstracted by OH• to form the **pre-RC3** complex. The **TS11** species shows an elongation of the C–Cl bond by 0.612 Å relative to the optimized bond length in TCFE (1.714 Å). In pathway **4**, the (*E*)-Cl-atom is abstracted by hydroxyl radicals to form the **pre-RC4**, and the **TS12** structure

demonstrates a substantial elongation of the C–Cl bond, breaking by 1.222 Å in comparison to the C–Cl bond length in TCFE molecule. Finally, in pathway **5**, the (*Z*)-Cl-atom is once again abstracted by $OH^{\bullet}$ radicals to form the **pre-RC5** complex. The **TS13** structure shows an even more significant elongation of the C–Cl bond, breaking by 1.336 Å compared to the optimized bond length of 1.705 Å.

The two C–Cl bonds that exist within TCFE are not identical. As indicated in Figure 1, the (*E*)-C–Cl bond distance is longer than the (*Z*)-C–Cl bond length by 0.004 Å. This suggests that, in the abstraction reaction, the hydroxyl radicals are more likely to quickly abstract the (*E*)-Cl atom compared to the (*Z*)-Cl atom.

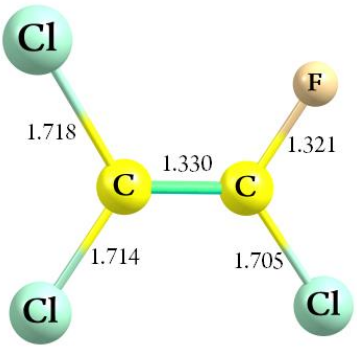

Figure 1. Optimized geometry of TCFE at the M06-2X method showing the different C–Cl bonds. (All bond distance dimensions are in Å)

Energetic and Thermodynamic Parameters

Table 1 presents the calculated total internal energies, enthalpies, and Gibbs free energies at 0 K and 298 K, for all the species involved in the reaction channels between TCFE and OH radicals, after considering zero-point vibrational energy (ZPVE) corrections. These thermodynamic properties provide insight into the feasibility of the reaction. Relative energies for all the species involved in the considered reaction at the CCSD(T)/aug-cc-pVTZ//M06-2X/6-311++G(d,p) theoretical level are tabulated in Table 1. The formation of pre-reactive complexes (pre-RC*i*, *i*=1–5) is a necessary step for all reaction channels, and these complexes have lower energies than the reactants. This can be attributed to the weak binding interactions between the isolated reactants. Specifically, the energies of the pre-RC1, pre-RC2, pre-RC3, pre-RC4, and pre-RC5 species lie around −3.53, −2.63, –0.36, –2.03, and –1.19 kcal mol^{-1} lower than the energy of the reactants, respectively, at the M06-2X method.

Addition of Hydroxyl Radicals to TCFE

When hydroxyl radicals are added onto the C1 and C2 positions of the C1=C2 bond of TCFE, two different energized adducts IM2 and IM6 [denoted as P1 and P2 as well in the previous section] are formed due to the non-equivalence of the carbon atoms at these positions (see Figure 2). In atmospheric conditions, the [TCFE–OH]• radical can undergo further reactions with molecular oxygen, forming the [TCFE-OH–O_2]• peroxy radical. As shown in Table 1, the M06-2X method is used to calculate the energy barriers, reaction energies, and thermodynamic parameters for these reactions.

Table 1 shows that both OH-addition pathways [**1**–**2**] to TCFE are exothermic ($\Delta H^o < 0$) and exoergic ($\Delta G^o < 0$) at the M06-2X level. However, reaction 1 (**R1**) has more negative ΔH^o and ΔG^o values than reaction **2** (**R2**), indicating that R1 is more feasible than R2. During the OH-addition pathways, hydroxyl radicals attack TCFE to form pre-reactive complexes, pre-RC1, and pre-RC2, for reactions **1**–**2**. The M06-2X [CCSD(T)] method shows that these pre-reactive complexes (RC...OH), at the entrance of the reaction have energies up to around 3.53 [2.72] kcal mol^{-1} lower than the reactants. The new interacting C…O bond distances in pre-RC1 and pre-RC2 are approximately 2.65 and 2.57 Å, respectively, showing a weak interaction at the M06-2X method is displayed in Figure 2.

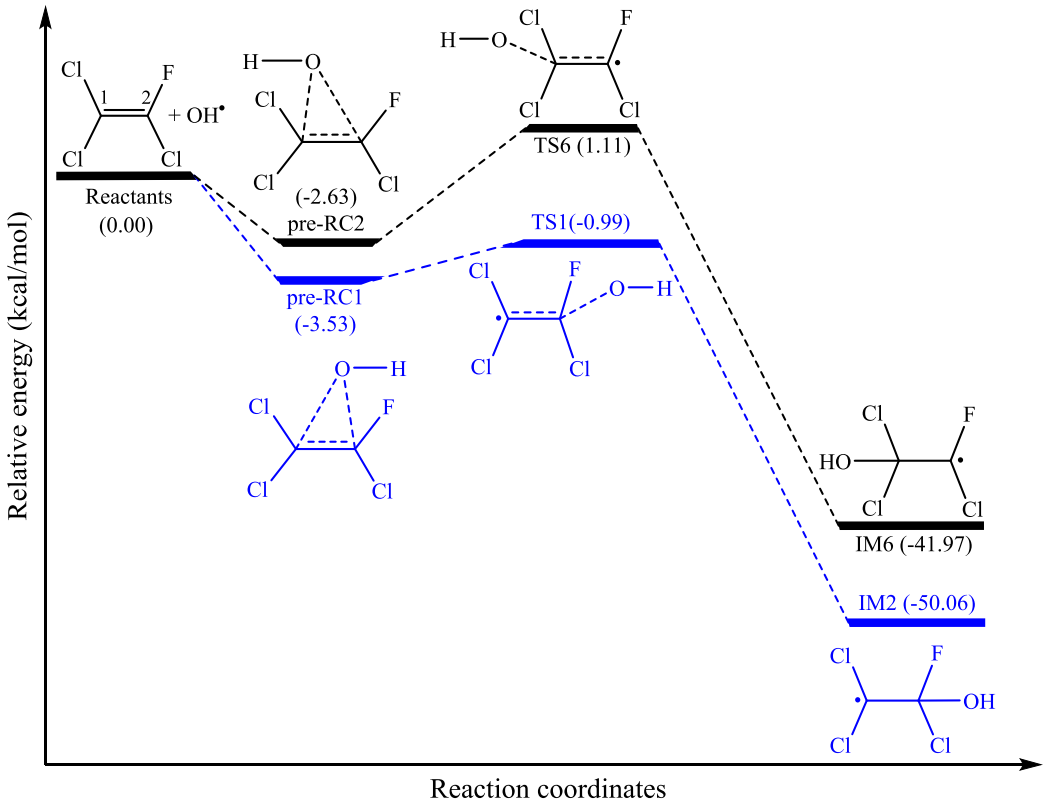

Figure 2. Potential energy profiles for the OH-addition channels (R1 and R2) at the M06-2X/6-311++G(d,p) level of theory.

Referring to the finding presented in Table 1, the TS1 structure in reaction **1** is found to be ~0.99 [1.59] kcal mol^{-1} lower than the reactants, while the TS2 structure in reaction **2** is located at ~1.11 [0.07] kcal mol^{-1} above the isolated reactants using the M06-2X [ROCBS-QB3//M06-2X/6–311++G(d,p)] method. The energy barrier associated with reaction **1** is therefore 2.1 kcal mol^{-1} lower than that for reaction **2** at the M06-2X method. This implies that the barrier height of TS1 is ~2.54 kcal mol^{-1} with respect to the pre-RC1 radical. As shown in Table 1, the reaction energy of the $^{\bullet}CCl_2$-C(OH)ClF radical is determined to be −50.06 [−51.41] kcal mol^{-1} at the M06-2X [CCSD(T)] level, which aligns with the findings for other fluorinated alkenes (as reported in references[21]).

The energy barrier associated with reaction **2** is measured to be approximately 3.74 kcal mol^{-1} concerning the pre-RC2 species. The energy of the $C(OH)Cl_2$–$C^{\bullet}ClF$ adducts is found to be around −41.97 [−42.81] kcal mol^{-1} using the M06-2X [CCSD(T)] method. The difference in energy barrier between the OH-addition reactions [TCFE+$OH^{\bullet}$→P*i*, *i*=1–2] suggests that the formation of the IM2 species has the lowest Gibbs free energy of activation ($\Delta G^{\dagger}$=7.79 kcal mol^{-1}) and will be kinetically favored over the production of the energized adducts IM6 (as nominated P2) (see Table 1). As shown in Figure 2, the formation of the IM2 species (via pathway **1**) is thermodynamically favored with the reaction enthalpy (ΔH_{298}) and Gibbs free energy (ΔG_{298}) being –51.21 and –41.11 kcal mol^{-1}, respectively.

Chlorine Atom Abstraction Pathways

The energy barrier for reaction **3** (**R3**), which involves chlorine atom (bonded to the C1 atom) abstraction by hydroxyl radicals, is around 36.77 (35.29) kcal mol^{-1} according to the M06-2X (ROCBS-QB3//M06-2X) method, with the associated products [HOCl+$^{\bullet}$CCl=CClF] having an energy of ~61.35 kcal mol^{-1}. Similarly, for reaction **4** (**R4**), which involves removing the other chlorine atom from C1, the energy barrier is around 36.13 (33.49) kcal mol^{-1} at the M06-2X (ROCBS-QB3//M06-2X) theoretical level, and the related products [HOCl+$^{\bullet}$CCl=CClF] have an energy of ~59.85 kcal mol^{-1}. Finally, the abstraction of chlorine from the C2 atom in TCFE requires activation and reaction energies of 41.48 [39.93] and 60.11 [60.13] kcal mol^{-1}, respectively, at the M06-2X [ROCBS-QB3//M06-2X] level.

Within the TCFE molecule, there are three different types of chlorine atoms, which provide the potential for three separate oxidation reactions. The M06-2X data shows the existence of three pre-reactive complexes: pre-RC3, pre-RC4, and pre-RC5, characterized by Cl3–O7, Cl4–O7, and Cl6–O7 bond distances of 2.999, 2.985, and 2.964 Å, respectively. At

the TS3–TS5 structures, the C–Cl and O–Cl bond lengths elongated compared to the equilibrium structure. Based on the optimized structures, it appears that the C–Cl bond experiences less stretching compared to the O–Cl bond. This suggests that transition states TS3–TS5 are more similar to the initial reactants than to the final products.

Table 1. The energetic and thermodynamic parameters for all stationary points involved in the examined pathways at the M06-2X, CCSD(T)/aug-cc-pVTZ//M06-2X, and ROCBS-QB3//M06-2X levels (P=1 bar, T=298 K), as well as T_1-diagnostic values for pathways **1**–**2** obtained from the M06-2X method.

Species \ Parameter	ΔE_{0K}	$\Delta H°_{298K}$	$\Delta G°_{298K}$	$\Delta E_{0K}^{\dagger}$	$\Delta H°_{298K}^{\dagger}$	$\Delta G°_{298K}^{\dagger}$	$\Delta S°_{298K}^{\dagger}$	T_1[c]
TCFE+OH$^{\bullet}$	0.000	0.000	0.000	0.000	0.000	0.000	0.000	
	R1: TCFE + OH → TS1 → $^{\bullet}CCl_2$–C(OH)ClF							
pre-RC1 [TCFE...OH]$^{\bullet}$	–3.525 [–2.381][a] (–2.718)[b]	–3.560 [–2.227][a]	3.904 [4.064][a]					0.0208
TS1 [TCFE...OH]$^{\bullet}$				–0.991 [–1.591][a] (–1.914)[b]	1.792 [–2.402][a]	7.786 [7.218][a]	–32.120	0.0315
IM2 [$^{\bullet}CCl_2$–C(OH)ClF]	–50.063 [–49.129][a] (–51.408)[b]	–51.208 [–50.216][a]	–41.106 [–40.633][a]					0.0154
	R2: TCFE + OH → TS2 → C(OH)Cl_2–C$^{\bullet}$ClF							
pre-RC2 [TCFE...OH]$^{\bullet}$	–2.632 [–1.449][a] (–2.097)[b]	–2.926 [–1.672][a]	5.175 [6.210][a]					0.0244
TS2 [TCFE...OH]$^{\bullet}$				1.111 [0.065][a] (–0.149)[b]	0.274 [–0.764][a]	9.969 [8.909][a]	–32.517	0.0315
IM6 [C(OH)Cl_2–C$^{\bullet}$ClF]	–41.968 [–40.020][a] (–42.813)[b]	–43.094 [–41.085][a]	–32.895 [–31.259][a]					0.0149
	R3: TCFE + OH → TS3 → HOCl + $^{\bullet}$CCl=CClF							
pre-RC3 [TCFE...OH]$^{\bullet}$	–0.362 [–1.048][a] (–1.744)[b]	–1.051 [–1.643][a]	8.020 [7.002][a]					
TS3 [TCFE...OH]$^{\bullet}$				36.771 [35.287][a] (35.511)[b]	36.227 [34.006][a]	42.590 [43.458][a]	–21.340	
P3 [HOCl + $^{\bullet}$CCl=CClF]	61.345 [59.826][a] (57.710)[b]	60.871 [59.397][a]	58.657 [57.095][a]					
	R4: TCFE + OH → TS4 → HOCl + $^{\bullet}$CCl=CClF							
pre-RC4 [TCFE...OH]$^{\bullet}$	–2.028 [–1.015][a] (–1.686)[b]	–2.596 [–1.596][a]	5.912 [7.021][a]					
TS4 [TCFE...OH]$^{\bullet}$				36.133 [33.488][a] (34.048)[b]	35.450 [31.865][a]	42.740 [41.235][a]	–24.450	

P4 [HOCl + $^{\bullet}$CCl=CClF]	59.853 [58.193][a] (56.233)[b]	59.305 [57.700][a]	57.220 [55.532][a]				
	R5: TCFE + OH → TS5 → HOCl + CCl_2=$^{\bullet}$CF						
pre-RC5 [TCFE...OH]$^{\bullet}$	−1.195 [−1.032][a] (−1.715)[b]	−1.824 [−1.620][a]	6.966 [7.012][a]				
TS5 [TCFE...OH]$^{\bullet}$				41.476 [39.930][a] (39.309)[b]	40.406 [37.782][a]	48.170 [49.183][a]	−26.031
P5 [HOCl + CCl_2=$^{\bullet}$CF]	60.114 [60.127][a] (58.112)[b]	59.558 [59.685][a]	57.431 [57.378][a]				

All the energies are in units of kcal mol^{-1}, except $\Delta S°$ which is in units of cal mol^{-1} K^{-1}.

[a] all data presented in "square brackets" were calculated using the ROCBS-QB3//M06-2X/6-311++G(d,p) method.
[b] all data in "parentheses" were calculated at the CCSD(T)/aug-cc-pVTZ//M06-2X/6-311++G(d,p) method.
[c] the T_1-diagnostic values were estimated using the ROCCSD(T)/6-31+G(d) method.

Comparison of OH-addition and Cl-abstraction Pathways

The results of this work indicate that the OH-addition pathways [**1**–**2**] are energetically favorable ($\Delta H < 0$) and thermodynamically spontaneous ($\Delta G < 0$). In contrast, the pathways involving the removal of chlorine atoms are energetically unfavorable ($\Delta H > 0$) and endoergic ($\Delta G > 0$). The fact that the Gibbs free energy of reaction (ΔG_r) for the degradation process has a negative value indicates that attacks by OH radicals at either the C1 or C2 positions are thermodynamically advantageous. Based on the M06-2X method, it has been determined that the most favorable reaction in terms of both thermodynamics (with a value of ΔE_{0K}= −50.06 kcal mol^{-1}) and kinetics (with a value of $\Delta G^{\dagger}$=7.79 kcal mol^{-1}) is the addition of OH to the C2 position.

The OH radicals attacking the C1 and C2 atoms exhibit the lowest Gibbs free energy of activation, with $\Delta G^{\dagger}$ values of 9.97 and 7.79 kcal mol^{-1}, respectively, at the M06-2X level. In contrast, the removal of chlorine atoms bonded to the C1 and C2 positions is associated with the highest Gibbs free activation energies, with $\Delta G^{\dagger}$ values exceeding 42.5 kcal mol^{-1} at the same level. Based on the lower activation energy of OH-addition reactions [**1–2**] in comparison to the removal of Cl-atom reactions [**3–5**], it can be inferred that the oxidation of TCFE by OH$^{\bullet}$ proceeds via OH-addition rather than Cl-abstraction reactions.

The reaction energies for pathways **1–2** are highly exothermic, ranging from –41.97 to –50.06 kcal mol^{-1}. In contrast, pathways **3–5** are endothermic, with energy ranges of 59.31 to 60.87 kcal mol^{-1} and reaction energies of 59.85 to 61.35 kcal mol^{-1}. Notably, the energy barriers for pathways **1–2** are significantly lower than those for pathways **3–5**, with a difference of 42.47 kcal mol^{-1}. This discrepancy in energy barriers indicates that OH-addition

processes are more importance than Cl-abstraction processes and occur at a significantly faster rate. OH-addition pathways have much lower activation energies (see Table 1). Due to the considerably higher barrier heights, all the Cl-abstraction reactions will not be discussed further. The results indicate that adducts [**P1**–**P2**] can be easily produced through pathways **1**–**2** and can subsequently react with molecular oxygen to form related peroxy radicals in the atmosphere.

Table 1 displays that the energy calculations performed using the M06-2X method are in agreement with those conducted at the CCSD(T)/aug-cc-pVTZ//M06-2X/6-311++G(d,p) level of theory. However, there are discrepancies in energy values between the M06-2X and CCSD(T) methods for the Cl-abstraction and OH-addition pathways, with differences of up to approximately 0.92 and 3.62 kcal mol^{-1}, respectively. It's worth noting that the difference is less significant for the OH-addition processes. Since the CCSD(T) method places the barrier for the TS1 species just above the energy of the associated pre-reactive complex, the M06-2X energies were used for the kinetic modeling analysis. Interestingly, the energy of the TS1 species leading to the IM2 species consistently appeared lower than that of the TS2 species leading to the IM6 species at both the M06-2X and CCSD(T) methods. The optimized structures of all the species involved in the primary reaction have been depicted in Figure S2 of the Supporting Information using the M06-2X/6-311++G(d,p) method.

Kinetic Parameters

The study examines the degradation reactions between TCFE and $OH^{\bullet}$ radicals. This includes analyzing the first pre-equilibrium between the reactants and the formation of the pre-RC. It is then followed by an irreversible step that leads to energized adducts as follows:[22]

$$\mathrm{TCFE} + \mathrm{OH}^{\bullet} \underset{k_{-1}}{\overset{k_1}{\rightleftharpoons}} \left[\mathrm{TCFE}\cdots\mathrm{OH}\right]^{\bullet}$$

$$\left[\mathrm{TCFE}\cdots\mathrm{OH}\right]^{\bullet} \xrightarrow{k_2} \left[\mathrm{TCFE}-\mathrm{OH}\right]^{\bullet}$$

since the entropy change for the reverse unimolecular reaction (k_{-1}) is greater than the entropy change for the formation of energized adducts (k_2).[22b] Thus, we must expected $k_{-1} >> k_2$, and the overall rate coefficient is given by

$$k_{\mathrm{overall}} = K_{\mathrm{eq}} \times k_2 \qquad (1)$$

where $K_c=k_1/k_{-1}$ denotes the pre-equilibrium constant between the reactants and the pre-RC. In the high-pressure limit, TST is utilized to calculate the rate constant specified by the unimolecular process.

$$k_2 = \kappa(T) \times \frac{\sigma k_B T}{h} \times \frac{Q_{TS}}{Q_{pre\text{-}RC}} \times \exp\left(-\frac{[E_{TS} - E_{pre\text{-}RC}]}{RT}\right) \quad (2)$$

where k_B and h are the Boltzmann and Planck constants, respectively. $Q_{pre\text{-}RC}$ and Q_{TS} represent the total molecular partition functions for the pre-reactive complex (pre-RC), and the transition state (TS) associated with the unimolecular dissociation reaction (step 2), respectively.[23] Also, $E_{pre\text{-}RC}$ and E_{TS} are the corresponding energies, including M06-2X/6-311++G(d,p) estimates for zero-point vibrational contributions. In equation 2, $\kappa(T)$ and σ denote the Eckart tunneling correction and reaction symmetry number characterizing step 2.

The computed branching ratios (BRs) represent the relative proportions of the OH-addition pathways [**1**–**2**] and are defined as BR(**1**)=[k_1/(k_1+k_2)] and BR(**2**)=[k_2/(k_1+k_2)], where k_1 and k_2 denote the rate constants for pathways **1** and **2**, respectively. TST was used to calculate the rate constant for each reaction and the overall rate coefficient ($k_{overall}$) for the OH-addition reactions at a P=1 bar and a temperature ranging from 250 to 450 K with 20 K intervals (see Figure 3 and Table 2). As previously predicted, it was observed that the rate constant for the reverse reaction, k_{-1}, was significantly larger than the rate coefficient for the second step, k_2, in the studied OH-addition pathways (see Table 2).

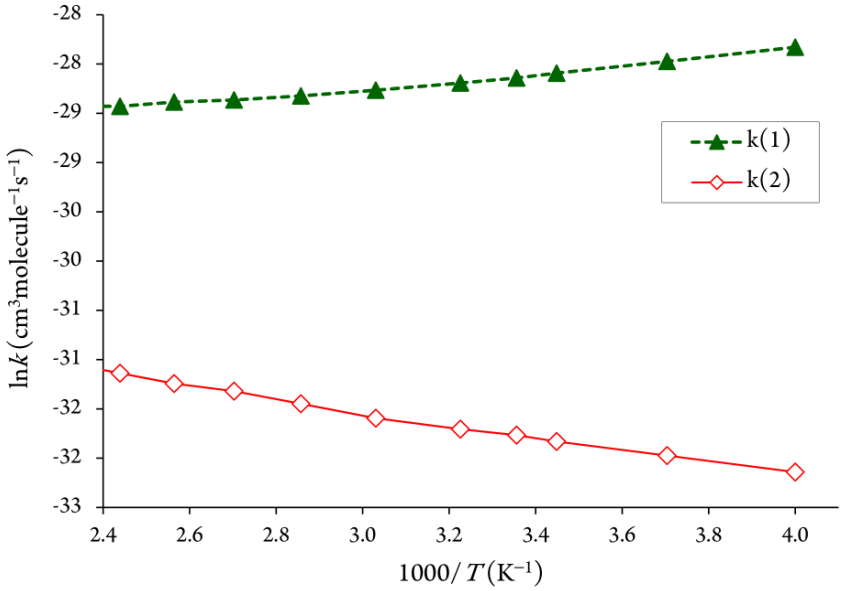

Figure 3. The Arrhenius plot of the calculated effective rate constants, k_{eff}, using TST.

The calculated BRs show that $OH^{\bullet}$ radicals attacks at the C1 and C2 positions resulting in consistently energized adducts are expected to be 1.32–7.76, and 92.24–98.68 %, respectively. As shown in Table 2, at higher temperatures, the percentage of pathway **1** decreases gradually, whereas the percentage of pathway **2** increases. At room temperature, the computed percentage branching ratios (% BR) for reactions **1** and **2** are 97.4% and 2.6%, respectively.

Our calculated kinetic rates for reactions **1** and **2** range from 8.2×10^{-13} to 4.4×10^{-13} and from 1.1×10^{-14} to 3.7×10^{-14} cm^3 $molecule^{-1}$ s^{-1}, respectively. As indicated in Figure 3 and Table 2, the TST data for the first bimolecular reaction step (TCFE+$OH^{\bullet}$→IM2) in reaction pathway **1** exhibit a negative temperature dependency, indicating a preference for OH-addition at the C2 position within the studied temperature range. In contrast, the TST rate constants for the initial bimolecular reaction step (TCFE+$OH^{\bullet}$→IM6) in reaction pathway **2** show a positive temperature dependency. The effect of tunneling seems to have a minor impact on the estimated rate constants and is not significant in practical terms. The Eckart correction factors for reaction pathways **1**–**2** vary from 1.1 to 1.4 within the specified temperature range. The temperature-dependent percentage branching ratios have also been calculated at the M06-2X level for temperature ranges of 250 to 450 K. As can be seen from Table 2, the individual Eckart rate coefficients for **R1** and **R2** reaction pathways are 6.0×10^{-13} and 1.6×10^{-14} cm^3 $molecule^{-1}$ s^{-1}, correspondingly, and the overall Eckart corrected rate constant is 6.2×10^{-13} cm^3 $molecule^{-1}$ s^{-1} (T=298 K).

While the calculated energy barrier for OH addition reactions at the C1 and C2 atoms differs by 2.1 kcal mol^{-1}, the kinetic rate constant for OH addition at the C2 atom is approximately 75.5 times faster than that of OH addition at the C1 atom across the studied temperature ranges. This significant difference can be attributed to the Gibbs free energy calculated for the attack at the C1 position, which is −32.90 [−31.09] kcal mol^{-1}. This value is approximately 8.2 [9.4] kcal mol^{-1} higher than the OH addition reaction at the C2 position at the M06-2X [CCSD(T)] level of theory.

Table 2. The calculated Eckart-corrected rate constants (units: unimolecular reactions in s^{-1}; bimolecular reactions in $cm^3molecule^{-1}s^{-1}$) for all studied OH-addition channels involved in the degradation of TCFE by $OH^{\bullet}$ in the temperature ranges of 250–450 K with branching ratios (%) calculated at the M06-2X/6-311++G(d,p) level of theory.

T (K)	Rate constants							Branching ratios		Tunneling factor	
	pre-RC1→R+OH$^{\bullet}$ k_{-1} (s^{-1})	pre-RC2→R+OH$^{\bullet}$ k_{-1} (s^{-1})	pre-RC1→IM2 k_{2a} (s^{-1})	pre-RC2→IM6 k_{2b} (s^{-1})	R+OH$^{\bullet}$→IM2 k(**1**)	R+OH$^{\bullet}$→IM6 k(**2**)	$k_{overall}$ [k(**1**)+k(**2**)]	BR(**1**)	BR(**2**)	κ(**1**)	κ(**2**)
250	1.35×10^{16}	1.7×10^{17}	2.9×10^{9}	6.0×10^{8}	8.2×10^{-13}	1.1×10^{-14}	8.3×10^{-13}	98.68	1.32	1.3	1.4
270	8.1×10^{15}	8.7×10^{16}	4.1×10^{9}	1.0×10^{9}	7.1×10^{-13}	1.3×10^{-14}	7.2×10^{-13}	98.20	1.80	1.3	1.4
290	5.3×10^{15}	4.8×10^{16}	5.7×10^{9}	1.7×10^{9}	6.3×10^{-13}	1.5×10^{-14}	6.5×10^{-13}	97.67	2.33	1.2	1.3
298	4.5×10^{15}	3.9×10^{16}	6.3×10^{9}	2.0×10^{9}	6.0×10^{-13}	1.6×10^{-14}	6.2×10^{-13}	97.40	2.60	1.2	1.3
310	3.6×10^{15}	2.9×10^{16}	7.4×10^{9}	2.5×10^{9}	5.7×10^{-13}	1.7×10^{-14}	5.9×10^{-13}	97.10	2.90	1.2	1.3
330	2.7×10^{15}	1.8×10^{16}	9.5×10^{9}	3.6×10^{9}	5.3×10^{-13}	1.9×10^{-14}	5.5×10^{-13}	96.54	3.46	1.2	1.2
350	2.0×10^{15}	1.2×10^{16}	1.2×10^{10}	4.9×10^{9}	5.0×10^{-13}	2.2×10^{-14}	5.2×10^{-13}	95.79	4.21	1.1	1.2
370	1.6×10^{15}	8.8×10^{15}	1.4×10^{10}	6.6×10^{9}	4.8×10^{-13}	2.5×10^{-14}	5.1×10^{-13}	95.05	4.95	1.1	1.2
390	1.3×10^{15}	6.46×10^{15}	1.7×10^{10}	8.5×10^{9}	4.7×10^{-13}	2.7×10^{-14}	5.0×10^{-13}	94.57	5.43	1.1	1.2
410	1.0×10^{15}	4.9×10^{15}	2.0×10^{10}	1.1×10^{10}	4.6×10^{-13}	3.0×10^{-14}	4.9×10^{-13}	93.75	6.25	1.1	1.1
430	8.6×10^{14}	3.8×10^{15}	2.3×10^{10}	1.3×10^{10}	4.5×10^{-13}	3.3×10^{-14}	4.8×10^{-13}	93.17	6.83	1.1	1.1
450	7.4×10^{14}	3.1×10^{15}	2.6×10^{10}	1.6×10^{10}	4.4×10^{-13}	3.7×10^{-14}	4.7×10^{-13}	92.24	7.76	1.1	1.1

Atmospheric Lifetime

There is currently no kinetic data available for the reaction between TCFE and OH. Photolysis and gas-phase reactions with atmospheric oxidants are utilized to eliminate volatile organic compounds from the environment. A previous study[16] has shown that halo-olefin oxidation products are eliminated from the atmosphere through wet and dry deposition, which can take several days to weeks. This study employed M06-2X calculations to approximate the atmospheric reaction lifetimes. The total rate coefficient for the reaction at a pressure of 1 bar and the room temperature was determined to be 6.2×10^{-13} cm^3 $molecule^{-1}$ s^{-1}, as displayed in Table 2. Achieving uniform distribution of gases in the atmosphere takes years. Thus, the estimated atmospheric lifetime of TCFE should be considered as an approximation.[24] Furthermore, determining the actual lifetime is difficult due to variations in the average daily concentration of OH radicals in the atmosphere, which can be influenced by a variety of factors, including different physiochemical locations, seasons, and other factors.[25] The atmospheric lifetimes (τ) and half-life time ($t_{1/2}$) of this reaction can be described based on the average [$OH^{\bullet}$] in the troposphere during a 12-hour day, which is 2.2×10^6 molecule cm^{-3},[26] as follows:

$$\tau = \frac{1}{k_{(\mathrm{TCFE+OH})} \times [\mathrm{OH}^{\bullet}]} \tag{3}$$

$$t_{\frac{1}{2}} = \frac{ln2}{k_{(\mathrm{TCFE+OH})} \times [\mathrm{OH}^{\bullet}]} \tag{4}$$

here, the estimated atmospheric lifetime and half-life time are nearly 8.49 and 5.88 days, respectively, where k represents the kinetic rate constant, and [OH] is the average concentration of hydroxyl radicals in the atmosphere. Consistent with the screening criteria of the Stockholm Convention,[27] organic pollutants as persistent organic pollutants (POPs) if they persist in the atmosphere for more than two days. Since CCl_2=CClF has a half-life time of more than two days, it is considered potentially persistent in the atmosphere. Indeed, it is important to note that the estimated atmospheric lifetime provided is only an approximation, as various factors such as physiochemical locations, seasonal changes, and other related factors can cause fluctuations in the average daily concentration of OH radicals to present in the atmosphere.[24] As a result, the estimated atmospheric lifetime of this reaction may differ from the actual value, and further studies are needed to accurately determine its environmental impact.[25]

Global Warming Potentials

Another criterion for assessing the impact on the troposphere is the global warming potential, which is defined as the measure of the amount of heat trapped by a greenhouse gas (GHG) in the atmosphere compared to carbon dioxide as a reference gas. An absolute GWP for TCFE ($AGWP_{TCFE}$), measured in W m^{-2} Year kg^{-1} over a specific time horizon (H in years), has been estimated based on scaled vibrational frequencies[28], denoted as ν_k, and their corresponding intensities (A_k) at the M06-2X/6-311++G(d,p) level of theory. The estimated lifetimes (τ_{OH}) were calculated using the Pinnock method (eq. 6)[29]

$$GWP_{TCFE}(H) = \frac{\int_o^H RF_{TCFE}(t)dt}{\int_o^H RF_{CO_2}(t)dt} = \frac{AGWP_{TCFE}(H)}{AGWP_{CO_2}(H)} = \frac{A\tau\left[1-\exp\left(-H/\tau\right)\right]}{AGWP_{CO_2}(H)} \quad (5)$$

For TCFE, where A represents the total instantaneous infrared radiative forcing (in W m^{-2} $ppbv^{-1}$), τ denotes the atmospheric lifetime, H is the time horizon, and $F(\nu_k)$ is the radiative forcing function per unit cross-section per wavenumber (in units of W m^{-2} $(cm^{-1})^{-1}$ (cm^2 $molecule^{-1})^{-1}$) evaluated at the scaled band center frequency.[29] The integrated radiative forcing up to H is given by:

$$A = \sum_k A_k F(\nu_k) \quad (6)$$

It is noted that to convert total infrared radiative forcing from per ppb to per kg, we can multiply it by $(M_{air}/M_{TCFE})\times(10^9/T_M)$, where M_{air} and M_{TCFE} represent the molecular weight of dry air (28.97 g/mol) and TCFE (148.9 g/mol), respectively, and T_M is the mean dry mass of the atmosphere (5.135×10^{18} kg).[30] The radiative efficiency of CO_2, given per mass, is 1.75×10^{-15} W m^{-2} kg^{-1}. The resulting AGWPs for CO_2 are 2.495×10^{-14}, 9.171×10^{-14} and 3.217×10^{-13} W m^{-2} year kg^{-1} CO_2 for time horizons of 20, 100 and 500 years, respectively.[31]

The calculated radiative effective $[A_kF(\nu_k)]$ for TCFE is estimated to be 0.25 W m^{-2} $ppbv^{-1}$ using the method proposed by Pinnock *et al.*[29] Due to the non-uniform mixture of gas in the atmosphere, a lifetime correction factor $f(\tau)$ must be considered by Hodnebrog *et al.*,[31] with the following formula

$$f(\tau) = \frac{a\tau^b}{1+c\tau^d} \quad (7)$$

where a, b, c, and d are constants with values of 2.962, 0.9312, 2.994, and 0.9302, respectively.[32] The curve is further constrained to ensure that $f(\tau)$ equals 0 for very short lifetimes and 1 for very long lifetimes.[31] In this study, the estimated atmospheric lifetime (τ)

is 0.023 years, resulting in a lifetime correction factor, $f(\tau)$ of 0.082. Consequently, the corrected radiative efficiency of TCFE is calculated as 0.25 W m^{-2} ppb^{-1}. A 10% increase is introduced to account for stratosphere temperature adjustments, leading to the final infrared radiative forcing value[31] of 0.275 W m^{-2} ppb^{-1}. By substituting these values into equation 6, the estimated GWP for TCFE is 9.61, 2.61, and 0.74 for time horizons of 20, 100, and 500 years, respectively. Due to the relatively small GWPs and shorter lifetimes obtained, it is evident that TCFE is expected to make a negligible contribution to global warming compared to the same amount of CO_2.

Ozone Depletion Potential

To assess the impact of volatile organic compounds (VOCs) on the atmosphere, various measures such as ODP, GWP, and radiative forcing efficiency and employed.[33] ODP refers to the extent to which a chemical can harm the ozone layer,[34] and to determine the ODP of compounds with varying lifespans, a semi-empirical method was used, which involved calculating the ODP of TCFE using trichlorofluoromethane ($CFCl_3$) as a reference compound. The latter has an ODP value of 1 and is currently the second most abundant atmospheric CFC.[35]

$$\mathrm{ODP}_{\text{perhaloalkenes}} = \frac{\tau_{\mathrm{TCFE}}}{\tau_{\mathrm{CFCl_3}}} \times \frac{M_{\mathrm{CFCl_3}}}{M_{\mathrm{TCFE}}} \times \frac{n_{\mathrm{Cl\,[TCFE]}}}{n_{\mathrm{Cl\,[CFCl_3]}}} \tag{8}$$

In the above equation, M_x refers to the molecular weight (where x can be either TCFE or $CFCl_3$), n represents the number of chlorine atoms in CTFE, and τ_x denotes the atmospheric lifetimes of individual species. The resulting ODP values obtained for these perhaloalkenes were found to be less than 2×10^{-3}, indicating that they have a minimal impact on the depletion of stratospheric ozone. The atmospheric lifetime of $CFCl_3$ is known to be 52 years,[2, 36] and its molecular weight (M_{CFCl3}) is 137.37 amu. In contrast, TCFE has an atmospheric lifetime of ~8.49 days when degraded by OH radicals, and its molecular weight (M_{TCFE}) is 147.91 amu. Using these values, the ODP value of TCFE was calculated to be 4.15×10^{-4}, further emphasizing its insignificance in contributing to the depletion of the stratospheric ozone layer.[33]

Photochemical Ozone Creation Potential

POCP is a crucial parameter that helps in determining the impact of an emitted species on the earth's atmosphere. The calculation is based on the potential of a species to produce O_3 by

reacting with oxidizing agents that are present in the atmosphere.[37] Previous studies, such as the one conducted by Wallington *et al.* have already assessed the POCP values of different olefins, with ethane's POCP value of 100 being used as a reference for POCP calculation.[38] The following equation shows a simplified assessment procedure for POCP calculation that only takes into account fundamental molecular properties:[39]

$$\varepsilon^{\mathrm{POCP}} = \alpha_1 \times \gamma_S \times \gamma_R^{\beta} \left(1 - \alpha_2 \times n_c\right) \tag{9}$$

where the values of three constants, namely α_1, α_2, and β, are given as 111, 0.04, and 0.5, respectively. The parameter γ_R corresponds to the reactivity-based index, while γ_S refers to the structure-based index for ozone formation. The formulas for calculating γ_S and γ_R can be found as follows:[37]

$$\gamma_S = \frac{n_B}{M} \times \frac{28}{6} \tag{10}$$

$$\gamma_R = \frac{k_{\mathrm{OH}}}{n_{\mathrm{B}}} \times \frac{6}{k_{\mathrm{OH}}^{\mathrm{ethane}}} \tag{11}$$

where n_C is the number of carbon atoms, and n_B denotes the total number of C–C and C–H bonds. The rate constant for ethane as a reference is $k_{\mathrm{OH}}^{\mathrm{ethane}} = 8.64 \times 10^{-12}\ \mathrm{cm^3\ molecule^{-1} s^{-1}}$. TCFE has a POCP of 2.99, which lies between the values of methane (0.6) and ethane (12.3).[39a] Earlier studies[39c, 40] indicate that methane and ethane have little impact on local air quality regulation due to their slow oxidation in the atmosphere. Hence, it can be concluded that TCFE is unlikely to contribute to tropospheric ozone formation and has a negligible impact on the atmosphere, which is consistent with the finding of Wallington *et al.*[24]

Photolysis of TCFE

To investigate the photolysis of TCFE in the gas phase, we determined the vertical excitation energy of TCFE, along with the energized adducts IM2 and IM6, which are produced as a result of the degradation reaction of TCFE initiated by hydroxyl radicals. These calculations were performed using the time-dependent density functional theory method at the M06-2X/6-311++G(d,p) level. The results are summarized in Table 3. According to previous studies[41], if the vertical excitation energy is less than 4.13 eV ($\lambda \approx 300$ nm), the molecule will undergo photolysis in sunlight. As indicated in Table 3, it is observed that photolysis in the troposphere is not possible for all species due to their excitation energies exceeding the tropospheric cut-off of 4.13 eV (~300 nm). Both TCFE and the energized adducts IM2 and

IM6 can potentially undergo photolysis at specific wavelengths, approximately 226, 272, and 253 nm, respectively.

Table 3. Vertical excitation energy, orbital transitions, absorption wavelength (λ), and oscillator strength (f) of TCFE and energized adducts IM2 and IM6 calculated at the TDDFT [M06-2X/6-311++G(d,p)] level of theory.

species	excitation energy (eV)	orbital transitions	absorption wavelength (nm)	oscillator strength (a.u.)
TCFE	5.4982	HOMO → LUMO+2	225.50	0.0000
IM2	4.5557	HOMO → LUMO+1	272.15	0.0022
IM6	4.8931	HOMO → LUMO+1	253.39	0.0033

Secondary Reactions

The $[R–OH]^{\bullet}$ adducts are prone to undergo isomerization or react with O_2, which is the 2nd most abundant component in the atmosphere,[42] as well as other trace species present in polluted areas, leading to their removal from the troposphere. NO_x has a significant impact on the oxidizing capacity of the atmosphere because it reacts with RO_2 radicals.[43] In polluted urban atmospheres with NO concentrations of ~1.23×10^{11} molecules cm^{-3}, the reaction between pollutants and $NO^{\bullet}$ radicals may have the potential to compete with the reaction with molecular oxygen.[44]

The isomerization of peroxy radicals is an essential reaction in the low-temperature combustion of hydrocarbon fuels.[45] As a result, the peroxy radicals that are produced from the relevant reaction will undergo isomerization at extremely low levels of [NO].[46] Consequently, the second pathway for the $[R\text{-}OH–O_2]^{\bullet}$ peroxy radical involves NO addition first, followed by NO_2 elimination, and finally the removal of H-atom by O_2 molecules. The rate-determining step is the NO_2 elimination process, which has the highest energy barrier. This reaction sequence occurs because the concentration of O_2 is higher than that of NO in the atmosphere.[47] NO is a critical component in the primary mechanism of O_3 formation in the troposphere. NO reacts with peroxy species, converting NO to NO_2, which is then photolyzed to form O_3 and regenerate NO.[48]

The energized adducts, known as $[CTFE\text{-}OH]^{\bullet}$ are unstable radicals and can readily react with O_2 in the atmosphere to oxidize the carbon adjacent to the OH. This implies that IM2 and IM6 species may be subjected to oxidation following this process. The energy released during the production of the energized adducts IM2 and IM6 with an energy of –50.06 and –41.97

kcal mol^{-1} could facilitate their further oxidation by O_2/NO under atmospheric conditions. The energized adducts of IM2/IM6 primarily react predominantly with O_2, resulting in the production of peroxy radicals with lower energy. These radicals then continuously combine with NO to form a different species. The reason for adding NO before O_2 is that the concentrations of O_2 molecule present in the atmosphere is higher than that of NO. It is worth emphasizing that the [TCFE-OH]$^{\bullet}$ radical undergoes isomerization to one of the several possible species through intramolecular transfer of the hydrogen, fluorine, or chlorine atoms, or conversion into associated species through migration of hydrogen, fluorine, or chlorine atoms.

The Atmospheric Pathway of the Energized Adducts IM2

We investigated eight possible unimolecular reaction channels for the primary adducts, $^{\bullet}CCl_2$–C(OH)ClF. The most energetically favorable channels were the 1,2-HF and 1,2-HCl loss channels, which formed $^{\bullet}CCl_2$–C(O)Cl and $^{\bullet}CCl_2$–C(O)F species, correspondingly, with exothermicity of –3.12 and –6.16 kcal mol^{-1} relative to the corresponding energized adducts. The production of epoxides through the channel involving 1,3-HCl-elimination and cyclization had an activation energy of 69.49 kcal mol^{-1}. In contrast, the channels involving 1,2-F- and 1,2-Cl-migration resulting in the production of $^{\bullet}CCl_2$–C(O)Cl and $^{\bullet}CCl_2$–C(O)F had barrier heights of 40.02 and 38.61 kcal mol^{-1}, respectively. The channel involving 1,3-H-migration resulted in the creation of $CHCl_2$–C($^{\bullet}$O)ClF and the barrier height for this process was 44.00 kcal mol^{-1}. In addition, the channels involving the loss of fluorine and chlorine atoms, CCl_2=C(OH)Cl and CCl_2=C(OH)F, were found to be endothermic by 60.70 and 29.69 kcal mol^{-1}, respectively, compared with the related energized adducts. The larger energy barriers of these channels mean that they require more energy to occur (see Table 4 and Figure S2, Supporting Information). There are three accessible reactions in the atmosphere among all possible channels of the main energized adducts (IM2), which are displayed in Table 4 as (*a*) the first reaction involves the loss of chlorine to produce CCl_2=C(OH)F, with an energy barrier of 16.37 kcal mol^{-1}. However, it is thermodynamically non-spontaneous, with a calculated ΔG_r value of 21.09 kcal mol^{-1} showing that it hardly occurs under atmospheric conditions; (*b*) the second reaction generates $^{\bullet}CCl_2$–C(O)Cl and $^{\bullet}CCl_2$–C(O)F radicals by undergoing 1,2-HF and 1,2-HCl-loss, with a barrier height of 36.81 and 17.73 kcal mol^{-1}, correspondingly; and (*c*) the third reaction occurs when IM2 reacts with O_2 to form [IM2–O_2]$^{\bullet}$ (denoted as IM3).

The process between energized adducts IM2 and O_2 is a spontaneous one that occurs under atmospheric conditions, with a strongly exothermic energy release of 21.31 kcal mol^{-1} and a ΔG_r value of −8.93 kcal mol^{-1}. This leads to the formation of the IM3 peroxy species. The reactions of the IM3 species with HO_2 and $NO^{\bullet}$ can follow either a terminating pathway, leading to the formation of a stable product, or a propagating pathway, resulting in the formation of an alkoxy radical, as depicted in Scheme 2. Previous studies suggest that the reaction rate for the peroxy radical + HO_2 is expected to be in the range of (10^{-11}–10^{-12}) cm^3 $molecule^{-1}$ s^{-1}, which is approximately one order of magnitude higher than the rate for the peroxy radical + NO reactions.[32] In atmospheric conditions with lower NO concentrations, such as unpolluted environments where [NO] is less than 10 ppb, the primary depletion mechanism for the peroxy radical is its reaction with the HO_2 radical.[49] Furthermore, IM3 peroxy radicals react with NO to yield a vibrationally excited [IM2-O_2–NO]$^{\bullet}$. Subsequently, [IM2-O_2–NO]$^{\bullet}$ directly decomposes to the [IM2–O]$^{\bullet}$ alkoxy radical (denoted as IM4), which can undergo two different reaction channels. The first channel involves the dissociation of a chlorine atom to form C(O)Cl–C(OH)ClF, which is a thermodynamically spontaneous, exothermic process with a barrier height of 4.34 kcal mol^{-1} and a ΔG_r of −17.04 kcal mol^{-1}.

The second channel involves the cleavage of the O–O bond to form phosgene and the $^{\bullet}$C(OH)ClF species (denoted as IM5), which can quickly react with molecular oxygen to produce CClFO and HO_2. Under typical atmospheric conditions, this reaction is energetically feasible and is barrierless and highly exothermic, releasing 29.46 kcal mol^{-1} (see Figure 1 and Table 4). The low energy barrier for the C–C bond breaking in this pathway is consistent with previous studies on non-fluorinated alkoxy radicals.[50]

It is noted that in previous studies,[51] the primary pathway of the RC($O^{\bullet}$)OR alkoxy radical was found to be the unimolecular decomposition by C–C bond cleavage. Instead, the unimolecular decomposition involving the breaking of the C–O bond was not considered to be very significant. Consequently, the significance of the reaction of the [TCFE-OH-$O^{\bullet}$] alkoxy radical with molecular oxygen, as well as its unimolecular isomerization, are also considered to be of lesser importance.

Table 4. Energy barriers (in kcal mol^{-1}) and reaction relative energies for the OH-addition pathways [**1**–**2**] at the M06-2X level. (P=1 bar, T=298 K)

species \ parameters	$\Delta E_{0K}^{\dagger}$	$\Delta H°_{298K}^{\dagger}$	$\Delta G°_{298K}^{\dagger}$	$\Delta S°_{298K}^{\dagger}$	ΔE_{0K}	$\Delta H°_{298K}$	$\Delta G°_{298K}$
TCFE + $OH^{\bullet}$	0.000	0.000	0.000	0.000	0.000	0.000	0.000
TCFE + $OH^{\bullet} \rightarrow [TCFE–OH_1]^{\bullet} \rightarrow$ *via*							
1,2-Cl-migration:→ $CCl_3–{}^{\bullet}C(OH)F$	38.612	38.405	39.123	–2.408	10.894	10.965	11.108
1,2-F-migration:→ $CCl_2F–{}^{\bullet}C(OH)Cl$	40.016	40.028	40.344	–1.059	8.138	8.175	8.122
1,2-HF-loss:→ $^{\bullet}CCl_2–C(O)Cl + HF$	36.803	36.805	36.654	0.505	–3.122	–1.886	–12.469
1,2-HCl-loss:→ $^{\bullet}CCl_2–C(O)F + HCl$	17.729	17.614	17.634	–0.071	–6.163	–5.145	–15.830
F-atom loss:→ $CCl_2=C(OH)Cl + F^{\bullet}$	40.016	40.028	40.344	–1.059	59.805	60.696	51.944
1,3-H-migration:→ $CHCl_2–C(^{\bullet}O)ClF$	43.997	43.586	44.439	–2.860	16.359	16.133	16.724
Cl-atom loss: → $CCl_2=C(OH)F + Cl^{\bullet}$	16.368	16.309	16.546	–0.794	28.990	29.693	21.089
1,3-HCl-loss with cyclization:→ $^{\bullet}CCl(O)CClF$+HCl	69.485	69.269	69.721	–1.517	37.204	37.912	28.043
TCFE + $OH^{\bullet} \rightarrow [TCFE–OH_2]^{\bullet} \rightarrow$ *via*							
1,2-Cl-migration: → $^{\bullet}C(OH)Cl–CCl_2F$	11.670	11.632	11.773	–0.476	–1.628	–1.628	–1.587
Cl-atom loss: → (*E*)-C(OH)Cl=CClF + $Cl^{\bullet}$	10.742	10.855	10.459	1.328	23.640	24.271	15.705
1,3-H-migration: → $C(^{\bullet}O)Cl_2–CHClF$	42.838	42.474	43.042	–1.908	12.818	12.610	13.083
Cl-atom loss: → (*Z*)-C(OH)Cl=CClF + $Cl^{\bullet}$	11.081	11.197	10.754	1.485	24.479	25.119	16.541
1,2-HCl-loss: → C(O)Cl–$^{\bullet}$CClF + HCl	12.478	12.270	12.408	–0.464	–6.896	–5.838	–16.729

The Atmospheric Pathway of the Energized Adducts IM6

Table 4 and Figure S3 in Supporting Information demonstrate that the minor adduct, $C(OH)Cl_2–{}^{\bullet}CClF$, can undergo similar fragmentation and rearrangement processes, resulting in five potential unimolecular reactions. The channels involving loss of chlorine, namely (*Z*)-C(OH)Cl=CClF and (*E*)-C(OH)Cl=CClF, were found to be endothermic by 25.12 and 24.27 kcal mol^{-1}, correspondingly. The 1,3-H-migration channel to form the $C(O^{\bullet})Cl_2–CHClF$ radical has a barrier height of 42.84 kcal mol^{-1}, whereas the 1,2-chlorine migration process leading to the $^{\bullet}C(OH)Cl–CCl_2F$ species has a barrier height of 11.67 kcal mol^{-1}. Finally, the formation of the $C(O)Cl–{}^{\bullet}CClF$ radical after the 1,2-HCl loss is the most easily accessible decomposition channel for this adduct, with an energy barrier of 12.48 kcal mol^{-1}.

The minor energized adduct, $C(OH)Cl_2–{}^{\bullet}CClF$, undergoes a similar fate as the main adduct, with the addition of O_2 through TS7b species to form the IM7b peroxy radical, which then forms the IM8 alkoxy radicals. Finally, the cleavage of the C–C bond results in the dominant channel, leading to the creation of $COCl_2$ and HO_2 radicals (see Table 4 and Figure S3, Supporting Information). The addition of oxygen molecules to the IM6 adducts is

barrierless (–26.17 kcal mol^{-1}) and leads to the related peroxy radical (denoted as IM7b) with an exothermicity of 28.55 kcal mol^{-1}. There are two successive steps identified for the rearrangement/ fragmentation of the IM7b species, with the highest barrier being 23.8 kcal mol^{-1}, which is considerably lower than the IM7b species (~ 15.36 kcal mol^{-1}).

An alternative, less energy-demanding pathway is available through the concerted elimination mechanism of $HO_2^{\bullet}$ (via transition state TS10). The activation energy for this process is calculated to be just 6.79 kcal mol^{-1} for the $C(OH)Cl_2–C(O^{\bullet})ClF$ alkoxy radical (denoted as IM8). This reaction results in the production of the $C(O)ClF–CCl_2(OH)\ldots O_2^{\bullet}$ complex, which subsequently dissociates without any energy barrier to yield carbonyl chloride fluoride and the $HO_2^{\bullet}$ radical. In the transition state labeled as TS9b, the C–C bond has broken with a bond distance of 1.767 Å. This transition state then proceeds to form a product complex, which has an enthalpy of approximately 19.43 kcal mol^{-1} below the isolated products. The energy of the free products is ~18.95 kcal mol^{-1} lower than that of the IM9 species (see Table S4, Supporting Information).

Before concluding the discussion of the reaction pathways for the energized adducts, it's important to note that the production of peroxy radicals from these adducts, which occurs due to OH attack on the C1 and C2 atoms, is highly exothermic with values of –30.06 and –28.55 kcal mol^{-1}, correspondingly. The peroxy radical formed at the C1 atom of the IM2 radicals is more likely to undergo O_2 addition than the C2 atom. According to the data presented in Scheme 2, Table 1, and Table S4 of the Supporting Information, the oxidation of NO to NO_2 by the $[TCFE\text{-}OH\text{-}O_2]^{\bullet}$ peroxy radical leaving $[TCFE\text{-}OH\text{-}O]^{\bullet}$ alkoxy radical is less exergonic and exothermic compared to the OH-initiated reaction followed by O_2 addition in both pathways. The alkoxy radicals produced during the reaction lead to the production of phosgene and carbonyl chloride fluoride, along with molecular oxygen. These reactions are very exothermic and exergonic, with values of 30.52 and 30.67 kcal mol^{-1}. This highlights the importance of the alkoxy radical in the degradation of TCFE. Among the reactions between the $C(^{\bullet}OO)Cl_2–C(OH)ClF$ peroxy radical and $NO^{\bullet}$, those involving O–O bond breaking of the peroxy radical by NO are the most thermodynamically favorable, with highly exothermic and exergonic values of 16.15 and 17.79 kcal mol^{-1}, correspondingly (see Table S4 in the Supporting Information).

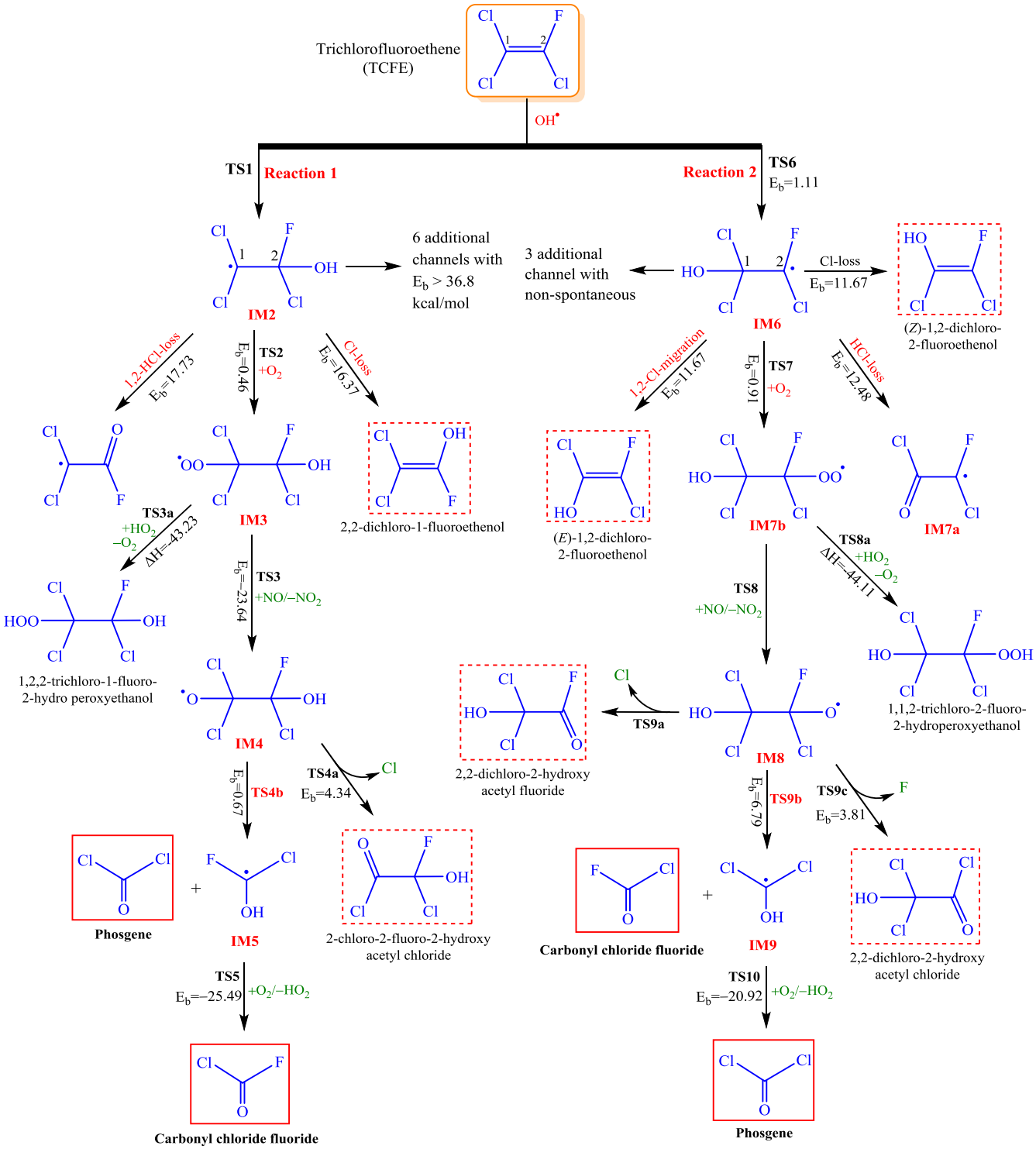

Scheme 2. Reaction pathways for OH addition onto C1 and C2 atoms in TCFE.

The dashed boxes represent speculated products, while the red boxes indicate observed products. (All reaction energy and energy barrier calculated at the M06-2X/6-311++G(d,p) level of theory are given in kcal mol^{-1})

Kinetic Study of the Main Energized Adducts

This section focused entirely on the subsequent processes of the IM2 species and did not consider the subsequent processes of the IM6 species that are associated with O_2 attacking the

C2 position. The overall rate coefficients were calculated at various temperatures and presented in Table S3 of the Supporting Information. Figure 4 shows an Arrhenius plot, which illustrates the TST calculations of all the available pathways for isomerization or decomposition of IM2 radicals at a pressure of 1 bar, based on M06-2X energy barrier assessments. The results indicate that the rate coefficients are temperature-dependent and increase as the temperature increases. As the temperature increases, the tunneling effect on the reaction rate constant decreases. This is because at higher temperatures, there is more thermal energy available to overcome the reaction barrier, and therefore tunneling becomes less significant in determining the reaction rate (see Figure 4 and Table S3 of the SI).

At the temperatures studied, the 1,2-HCl-loss process is found to be the most favorable pathway for the formation of HCl and $^{\bullet}CCl_2$–C(O)F species compared to the formation of other products. The rate constants for this process increase slowly as the temperature is raised, likely due to the presence of positive energy barriers.

In this section, the focus was solely on the subsequent processes of the IM2 species, and the kinetic study did not consider the follow-up processes of the [TCFE-OH]$^{\bullet}$ radical related to O_2 attacking the C2 position. The supplementary material contains Table S4, which presents the overall rate coefficients that were computed at various temperatures. Figure 4 depicts an Arrhenius plot that illustrates the TST estimates calculated at a pressure of 1 bar for all of the available isomerization or decomposition pathways of the energized adducts IM2, using the M06-2X energy barrier estimations.

Table 5. The measured TST branching ratios for the considered pathways (P = 1 bar).

Temperature / Reaction	T (K)				
	250	298	350	410	450
1,2-HCl-loss:→ $^{\bullet}CCl_2$–C(O)F + HCl	88.46	84.91	81.62	78.52	76.91
Cl-atom loss: → CCl_2=C(OH)F + Cl$^{\bullet}$	11.54	15.09	18.38	21.48	23.09
1,2-HF-loss:→ $^{\bullet}CCl_2$–C(O)Cl + HF	8.11×10^{-14}	1.77×10^{-11}	1.20×10^{-09}	4.31×10^{-08}	2.80×10^{-07}
1,2-Cl-migration:→ CCl_3–$^{\bullet}$C(OH)F	7.00×10^{-19}	9.67×10^{-16}	2.60×10^{-13}	2.83×10^{-11}	3.24×10^{-10}
1,2-F-migration:→ CCl_2F–$^{\bullet}$C(OH)Cl	8.00×10^{-20}	1.80×10^{-16}	7.03×10^{-14}	1.05×10^{-11}	1.42×10^{-10}
F-atom loss:→ CCl_2=C(OH)Cl + F$^{\bullet}$	7.81×10^{-20}	2.06×10^{-16}	7.42×10^{-14}	2.83×10^{-11}	2.02×10^{-10}
1,3-H-migration:→ $CHCl_2$–C(O$^{\bullet}$)ClF	1.76×10^{-20}	3.46×10^{-17}	1.25×10^{-14}	1.78×10^{-12}	2.35×10^{-11}
HCl-loss with cyclization:→ $^{\bullet}$CCl(O)CClF + HCl	3.46×10^{-44}	6.31×10^{-37}	2.58×10^{-31}	1.30×10^{-26}	3.56×10^{-24}

Based on the findings, it appears that the rate constants are affected by temperature and that they increase as the temperature rises. Additionally, the tunneling effect on the reaction

rate decreases as the temperature increases, as shown in Figure 4 and Table S4 of the SI. At the studied temperatures, the 1,2-HCl-loss pathway appears to be the most favorable reaction for the formation of HCl and $^{\bullet}CCl_2$–C(O)F compared to the other products. Due to the presence of positive energy barriers, the rate constants gradually increase slowly as the temperature is raised.

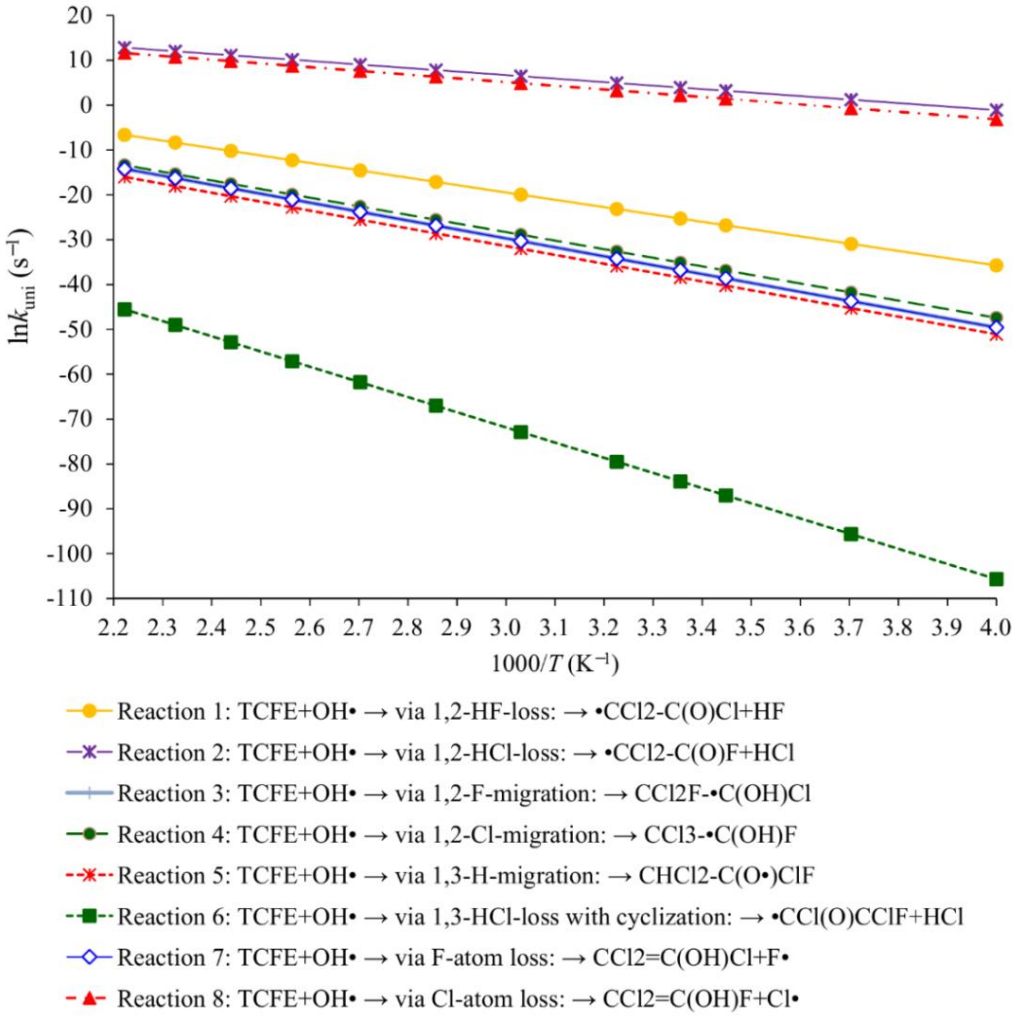

Figure 4. Arrhenius plot of the TST unimolecular rate constants derived using the M06-2X method.

According to Table 5, it was expected that the rate constant for the Cl-atom loss mechanism, which produces CCl_2=C(OH)F and has a barrier height of 16.37 kcal mol^{-1} (Table 5) would be greater than the kinetic rates for the other pathways. However, the 1,2-HCl-loss process was found to be more favorable from a kinetic viewpoint, which can be attributed to the entropy differences between the reactions (see Table S4, Supporting Information). It should be noted that for the other processes, except for the 1,2-HCl-loss process, the much higher energy barrier resulted in a significant difference in the rate constant in some cases. Table 5 presents the TST branching ratios for the different pathways investigated under conditions of

1 bar pressure and temperatures ranging from 250 K to 450 K. The data shows that the dominant reaction mechanism involves the production of HCl and $^{\bullet}CCl_2$–C(O)F radical via the 1,2-HCl-loss pathway, which is consistent with the energy profile and TST kinetic rate coefficients. As the temperature increases, the branching ratios for the other reactions gradually increase.

Conclusions

Our study was primarily concerned with investigating the processes that take place during the degradation of trichlorofluoroethene (TCFE) initiated by $OH^{\bullet}$ at atmospheric conditions. To optimize geometries and examine frequencies of all stationary points located on the potential energy surfaces, we employed the M06-2X/6-311++G(d,p) level. In addition, we carried out calculations of single-point energies utilizing the CCSD(T) approach together with the aug-cc-pVTZ basis set.

We employed the TST to determine the bimolecular rate coefficients and found that the energized adduct $[TCFE–OH]^{\bullet}$ is formed through a bimolecular reaction step. Under standard conditions of 1 bar pressure and room temperature, the initial reaction step is significantly exergonic, and the consistent transition states are placed below the isolated reactants. This phenomenon occurs because of the formation of weak pre-reactive complexes $[TCFE…OH]^{\bullet}$, which yields an effective negative activation energy of approximately –0.99 kcal mol^{-1} for reaction **1** [**R1**], which leads to the $^{\bullet}CCl_2$–C(OH)ClF species. On the other hand, for reaction **2** [**R2**] resulting in the C(OH)Cl_2–$^{\bullet}$CClF species, the initial bimolecular reaction step has a positive activation energy of around 1.11 kcal mol^{-1}, as determined by the M06-2X methodology.

After the formation of the energized adduct, a highly endergonic unimolecular reaction step occurs. According to the observed branching ratios, the most predominant outcome of the investigated reaction is the $^{\bullet}CCl_2$–C(OH)ClF radical. TCFE has an estimated lifetime of ~8.49 days in the presence of OH radicals at levels found in the troposphere, highlighting the significance of measuring its distribution and conversion in the atmosphere. Furthermore, the GWPs of TCFE for time horizons of 20, 100, and 500 years were calculated as 9.61, 2.61, and 0.74, respectively, with a photochemical ozone creation potential (POCP) of 2.99. The very low GWP values of TCFE indicate its negligible contribution to global warming and an

insignificant environmental impact. Furthermore, the POCP value of TCFE suggests that it has a negligible influence on tropospheric ozone formation following its emission.

Time-dependent density functional theory calculations show that the energized adducts produced from the degradation reaction of TCFE initiated by OH radicals are unable to photolysis under sunlight in the UV and visible spectrum.

Based on our theoretical calculations, we have found that the potential barriers for addition reactions are lower compared to isomerization reactions. This indicates that isomerization reactions are unlikely to occur in the atmosphere. Consequently, we suggest that "phosgene" and "carbonyl chloride fluoride" are the primary stable end-products of TCFE degradation through hydroxyl radicals in the atmosphere. Findings herein shall be useful in efforts that aim to underpin the fate of chlorofluorocarbons (CFCs) in the atmosphere.

Theoretical Section

The computations in this research were carried out using the Gaussian 16 software program.[52] The molecular structures were visually analyzed using the ChemCraft program [53]. DFT was utilized for geometry optimizations and vibrational frequency calculations of all relevant stationary points, employing the M06-2X functional[54] and the 6-311++G(d,p) basis set that includes enough polarization and diffuse functions. The M06-2X approach is recognized for its ability to provide accurate outcomes in determining the mechanisms and kinetics of atmospheric reactions.[55] This particular functional method exhibits strong performance in predicting barrier heights and providing reliable results for thermochemistry and kinetics, without increasing the computational cost.[32] The calculated harmonic frequencies were scaled by a factor of 0.97.[56] The electronic absorption spectra for the dissociated states of TCFE in the gas phase were computed through TDDFT calculations. These calculations were carried out at the M06-2X/6-311++G(d,p) level, which is considered and applicable method for assessing the properties of molecules in their excited states.[57] Further single-point energy calculations were performed using the CCSD(T) method. The geometries were optimized using the M06-2X/6-311++G(d,p) level, and the CCSD(T) calculations employed the larger aug-cc-pVTZ basis set. The CCSD(T) method is considered the gold standard for *ab initio* methods in atmospheric chemistry and is widely used in such studies.[58]

We computed electronic energies using the restricted open-shell complete basis set model chemistry for open-shell species (ROCBS-QB3), excluding the empirical correction term,

which partially reduces the impact of spin contamination.[59] To validate and crosscheck the thermodynamic findings at the M06-2X level, we conducted single-point energy calculations for all optimized stationary points using the ROCBS-QB3//M06-2X/6-311++G(d,p) method, along with the IOP(1/7=100000) keywords to exclude optimization and frequency calculations at the B3LYP level of the ROCBS-QB3 method. We utilized the T_1-diagnostics [60] at the ROCCSD/6-31+G(d') level with the M06-2X geometries to assess the multi-reference character of the CCSD(T) wavefunctions. Table 1 displays the T_1-diagnostic values for all studied reaction species, including the energized adducts and transition states, which were calculated to confirm the suitability of the single-reference method for energy structure calculations. The T_1-diagnostic values for IM*x* (*x*=2,6) and TS*y* (*y*=1,2) were around 0.015 and 0.032, respectively, which confirms the reliability of utilizing the single-reference method.[61] Single-reference calculations are considered reliable when the T_1 diagnosis is equal to or less than 0.044.[55d, 62]

To verify whether the identified transition state (TS) structures are linked to the reactants and relevant products, we performed intrinsic reaction coordinate (IRC) calculations[63] in both directions along the examined reaction channels, using the M06-2X approach.[64]

Kinetic rate coefficients at the high-pressure limits were utilized by employing TST, with activation energies (E_a) estimated using the M06-2X method that included contributions from ZPVE, as described in[65]

$$k_{\mathrm{TST}} = \kappa(T)\frac{\sigma k_B T}{h} V_m(T)\frac{Q_{TS}^{\dagger}}{Q_A \times Q_B}\exp\left(-E_a/RT\right) \qquad \text{(bimolecular reactions)} \tag{12}$$

$$k_{\mathrm{TST}} = \kappa(T)\frac{\sigma k_B T}{h}\frac{Q_{TS}^{\dagger}}{Q_A}\exp\left(-E_a/RT\right) \qquad \text{(unimolecular reactions)} \tag{13}$$

The definitions of all the parameters used in the above equations have been explained in our previous papers.[55] The Eckart tunneling correction, $\kappa(T)$ is a widely used method for including the effects of quantum tunneling in reaction rate calculations based on TST. It takes into account the potential energy barrier height, the mass of the reaction species, and the vibrational frequencies of the TS. We calculated the kinetic rate coefficients using the Eyringpy code,[66] which includes the Eckart tunneling correction[67] as follows

$$\kappa_{\mathrm{Eckart}}(T) = \frac{\exp\left(\Delta H_f^{\neq,0K}/k_{\mathrm{B}}T\right)}{k_{\mathrm{B}}T}\int_{\mathrm{o}}^{\infty} p(E)\exp\left(-E/k_{\mathrm{B}}T\right)dE \tag{14}$$

where $\Delta H_f^{\neq,0K}$ represents the zero-point corrected energy barriers in the forward direction, and $p(E)$ denotes the probability of transmission through the one-dimensional barrier at energy E.[55e]

Supporting Information

Supporting information file is available with the article through the web address.

Acknowledgments

Financial support of this study from Gdańsk University of Technology by the CHR-K.5147.2022 grant under the Nobelium Fellowship Grant-"Excellence Initiative-Research University" program is gratefully acknowledged. Computations were carried out using the computers of the Center of Informatics at the Tricity Academic Supercomputer & Network. The authors extend their gratitude to the anonymous referees for their stimulating feedback and relevant comments.

Keywords:

Atmospheric lifetime • global warming potentials • rate coefficient • POCP • Trichlorofluoroethene.

References

[1] a) J. Houghton, D. Albritton, M. Allen, A. Baede, J. Church, U. Cubasch, D. Xiaosu, D. Yihui, D. Ehhalt, C. Folland, in *Climate Change 2001: The Scientific Basis. Contributions of Working Group I to the Third Assessment Report of the Intergovernmental Panel on Climate Change*, Cambridge University Press, **2001**, pp. 1-20; b) V. Papadimitriou, *Journal of Science Education and Technology* **2004**, 299-307; c) U. N. E. P. O. Secretariat, *Handbook for the Montreal Protocol on Substances that Deplete the Ozone Layer*, UNEP/Earthprint, **2006**.

[2] J. B. Burkholder, R. Cox, A. Ravishankara, *Chem. Rev.* **2015**, *115*, 3704-3759.

[3] W.-T. Tsai, *Chemosphere* **2005**, *61*, 1539-1547.

[4] N. K. Gour, R. C. Deka, S. Paul, *New J. Chem.* **2020**, *44*, 3434-3444.

[5] M. Mashino, M. Kawasaki, T. Wallington, M. Hurley, *J.Phys. Chem. A* **2000**, *104*, 2925-2930.

[6] P. A. Domenico, F. W. Schwartz, *Physical and Chemical Hydrogeology*, John Wiley & sons, **1997**.

[7] E. A. Maull, H. J. Clewell, *Toxicology in Risk Assessment*, **2000**.

[8] K. J. Hageman, J. D. Istok, J. A. Field, T. E. Buscheck, L. Semprini, *Environ. Sci. Technol.* **2001**, *35*, 1729-1735.

[9] S. Vancheeswaran, R. U. Halden, K. J. Williamson, J. D. Ingle, L. Semprini, *Environ. Sci. Technol.* **1999**, *33*, 1077-1085.

[10] N. Bonvallot, P. Harrison, M. Loh, in *WHO Guidelines for Indoor Air Quality: Selected Pollutants*, World Health Organization, **2010**.
[11] a) C. E. P. Act, P. S. List, *Priority Substances List Assessment Report, Minister of Supply and Services, Canada* **1993**; b) T. O. Wiedmann, B. Guethner, T. J. Class, K. Ballschmiter, *Environ. Sci. Technol.* **1994**, *28*, 2321-2329.
[12] T. J. Wallington, W. F. Schneider, J. Sehested, O. J. Nielsen, *Faraday Discuss.* **1995**, *100*, 55-64.
[13] W. Kohn, L. J. Sham, *Phys. Rev.* **1965**, *140*, A1133.
[14] a) H. Eyring, *J. Chem. Phys.* **1935**, *3*, 107-115; b) H. S. Johnston, *Gas Phase Reaction Rate Theory, Vol. 82*, Ronald Press, New York, **1966**; c) K. J. Laidler, M. C. King, *J. Phys. Chem* **1983**, *87*, 2657-2664; d) E. E. e. Nikitin, *Theory of Elementary Atomic and Molecular Processes in Gases*, Oxford, Clarendon Press, **1974**; e) D. Rapp, *Statistical Mechanics*, Holt, Rinehart and Winston, **1972**; f) R. E. Weston, H. A. Schwarz, *Chemical Kinetics*, Prentice Hall, **1972**.
[15] T. H. Dunning Jr, *J. Chem. Phys.* **1989**, *90*, 1007-1023.
[16] J. Noga, R. J. Bartlett, *J. Chem. Phys.* **1987**, *86*, 7041-7050.
[17] E. Gross, J. Dobson, M. Petersilka, *Density Functional Theory II: Relativistic and Time Dependent Extensions* **2005**, 81-172.
[18] J. R. Alvarez-Idaboy, N. Mora-Diez, R. J. Boyd, A. Vivier-Bunge, *J. Am. Chem. Soc.* **2001**, *123*, 2018-2024.
[19] C.-W. Zhou, A. M. Mebel, X.-Y. Li, *J. Phys. Chem. A* **2009**, *113*, 10667-10677.
[20] a) N. Agmon, R. Levine, *Chem. Phys. Lett.* **1977**, *52*, 197-201; b) G. S. Hammond, *J. Am. Chem. Soc.* **1955**, *77*, 334-338.
[21] a) H. Ai, L. Zhang, A. K. Chang, H. Wei, Y. Che, H. Liu, *J. Mol. Model.* **2014**, *20*, 1-10; b) L.-l. Ai, X.-m. Duan, J.-Y. Liu, *Comput. Theor. Chem.* **2013**, *1013*, 15-22; c) M. Balaganesh, B. Rajakumar, *J. Mol. Graph. Model.* **2014**, *48*, 60-69; d) V. Saheb, N. Y. Pourhaghighi, *J. Phys. Chem. A* **2014**, *118*, 9941-9950.
[22] a) V. H. Uc, J. R. Alvarez-Idaboy, A. Galano, A. Vivier-Bunge, *J. Phys. Chem. A* **2008**, *112*, 7608-7615; b) D. Singleton, R. Cvetanovic, *J. Am. Chem. Soc.* **1976**, *98*, 6812-6819.
[23] M. A. Mahmoud, A. Shiroudi, M. A. Abdel-Rahman, M. F. Shibl, S. Abdel-Azeim, A. M. El-Nahas, *Comput. Theor. Chem.* **2021**, *1196*, 113119.
[24] T. Wallington, M. S. Andersen, O. Nielsen, *Chemosphere* **2015**, *129*, 135-141.
[25] M. J. Kurylo, V. L. Orkin, *Chem. Rev.* **2003**, *103*, 5049-5076.
[26] R. Prinn, R. Weiss, B. Miller, J. Huang, F. Alyea, D. M. Cunnold, P. Fraser, D. Hartley, P. Simmonds, *Science* **1995**, *269*, 187-192.
[27] C. Li, S. Zheng, J. Chen, H.-B. Xie, Y.-N. Zhang, Y. Zhao, Z. Du, *Chemosphere* **2018**, *201*, 557-563.
[28] I. Alecu, J. Zheng, Y. Zhao, D. G. Truhlar, *J. Chem. Theory Comput.* **2010**, *6*, 2872-2887.
[29] S. Pinnock, M. D. Hurley, K. P. Shine, T. J. Wallington, T. J. Smyth, *J. Geophys. Res. Atmos.* **1995**, *100*, 23227-23238.
[30] K. E. Trenberth, L. Smith, *J. Clim.* **2005**, *18*, 864-875.
[31] Ø. Hodnebrog, M. Etminan, J. Fuglestvedt, G. Marston, G. Myhre, C. Nielsen, K. P. Shine, T. Wallington, *Rev. Geophys.* **2013**, *51*, 300-378.
[32] R. Bhuvaneswari, K. Senthilkumar, *New J. Chem.* **2020**, *44*, 2070-2082.
[33] P. M. Cometto, R. A. Taccone, J. D. Nieto, P. R. Dalmasso, S. I. Lane, *ChemPhysChem* **2010**, *11*, 4053-4059.
[34] J. Zhang, D. J. Wuebbles, D. E. Kinnison, A. Saiz-Lopez, *J. Geophys. Res. Atmos.* **2020**, *125*, e2020JD032414.

[35] S. Solomon, D. L. Albritton, *Nature* **1992**, *357*, 33-37.
[36] L. Carpenter, S. Reimann, J. Burkholder, C. Clerbaux, B. Hall, R. Hossaini, J. Laube, S. Yvon-Lewis, *World Meteorological Organization Geneva*, **2014**.
[37] P. Gupta, B. Rajakumar, *J. Fluor. Chem.* **2019**, *222*, 31-45.
[38] T. Wallington, M. S. Andersen, O. Nielsen, *Atmos. Environ.* **2010**, *44*, 1478-1481.
[39] a) M. Baasandorj, A. Ravishankara, J. B. Burkholder, *J. Phys. Chem. A* **2011**, *115*, 10539-10549; b) R. Derwent, M. Jenkin, S. Saunders, *Atmos. Environ.* **1996**, *30*, 181-199; c) R. G. Derwent, M. E. Jenkin, S. M. Saunders, M. J. Pilling, *Atmos. Environ.* **1998**, *32*, 2429-2441.
[40] M. Jenkin, R. Derwent, T. Wallington, *Atmos. Environ.* **2017**, *163*, 128-137.
[41] a) G. Manonmani, L. Sandhiya, K. Senthilkumar, *Environ. Sci. Pollut. Res*. **2020**, *27*, 12080-12095; b) F.-Y. Bai, X. Wang, Y.-Q. Sun, X.-M. Pan, *RSC Adv.* **2015**, *5*, 88087-88095; c) Y. Tang, M. Hanrath, C. J. Nielsen, *Phys. Chem. Chem. Phys.* **2012**, *14*, 16365–16370.
[42] X. Zeng, Y. Wang, *Chemosphere* **2018**, *212*, 548-553.
[43] a) A. Gaur, S. Tripathi, V. Kanawade, V. Tare, S. Shukla, *J. Atmos. Chem.* **2014**, *71*, 283-301; b) I. Mavroidis, M. Ilia, *Atmos. Environ.* **2012**, *63*, 135-147; c) C. Stroud, S. Madronich, E. Atlas, B. Ridley, F. Flocke, A. Weinheimer, B. Talbot, A. Fried, B. Wert, R. Shetter, *Atmos. Environ.* **2003**, *37*, 3351-3364; d) Y. Sun, L. Wang, Y. Wang, L. Quan, L. Zirui, *Sci. Total Environ.* **2011**, *409*, 933-940.
[44] F. Ma, Z. Ding, J. Elm, H.-B. Xie, Q. Yu, C. Liu, C. Li, Z. Fu, L. Zhang, J. Chen, *Environ. Sci. Technol.* **2018**, *52*, 9801-9809.
[45] D. R. Glowacki, M. J. Pilling, *ChemPhysChem* **2010**, *11*, 3836-3843.
[46] L. Sandhiya, S. Ponnusamy, K. Senthilkumar, *RSC Adv.* **2016**, *6*, 81354-81363.
[47] Y. Liu, W. Wang, *Comput. Theor. Chem.* **2021**, *1197*, 113137.
[48] R. Atkinson, *Atmos. Environ.* **2000**, *34*, 2063-2101.
[49] a) J. J. Orlando, G. S. Tyndall, *Chem. Soc. Rev.* **2012**, *41*, 6294-6317; b) J. J. Orlando, G. S. Tyndall, T. J. Wallington, *Chem. Rev.* **2003**, *103*, 4657-4690.
[50] A. Mellouki, G. Le Bras, H. Sidebottom, *Chem. Rev.* **2003**, *103*, 5077-5096.
[51] a) E. C. Tuazon, S. M. Aschmann, R. Atkinson, *Environ. Sci. Technol.* **1998**, *32*, 3336-3345; b) K. Stemmler, W. Mengon, D. J. Kinnison, J. A. Kerr, *Environ. Sci. Technol.* **1997**, *31*, 1496-1504; c) K. Stemmler, W. Mengon, J. A. Kerr, *Environ. Sci. Technol.* **1996**, *30*, 3385-3391; d) J. A. Barrera, M. d. l. A. Garavagno, P. R. Dalmasso, R. A. Taccone, *Atmos. Environ.* **2019**, *202*, 28-40; e) S. M. Aschmann, P. Martin, E. C. Tuazon, J. Arey, R. Atkinson, *Environ. Sci. Technol.* **2001**, *35*, 4080-4088; f) S. M. Aschmann, J. Arey, R. Atkinson, *Environ. Sci. Technol.* **2011**, *45*, 6896-6901.
[52] M. J. Frisch, M. J. Frisch, G. W. Trucks, H. B. Schlegel, G. E. Scuseria, M. A. Robb and J. R. Cheeseman, et al., *Gaussian 16, Revision C.01*, Gaussian, Inc., Wallingford CT, **2019**.
[53] G. A. Zhurko, *Chemcraft Program v. 1.6.*, **2014**. https://www.chemcraftprog.com.
[54] a) Y. Zhao, D. G. Truhlar, *Theor. Chem. Acc.* **2008**, *120*, 215-241; b) Y. Zhao, D. G. Truhlar, *Acc. Chem. Res.* **2008**, *41*, 157-167.
[55] a) S. Safari Balsini, A. Shiroudi, F. Hatamjafari, E. Zahedi, K. Pourshamsian, A. R. Oliaey, *Phys. Chem. Chem. Phys.* **2023**, *25*, 13630-13644; b) A. Karton, A. Tarnopolsky, J.-F. Lamére, G. C. Schatz, J. M. Martin, *J. Phys. Chem. A* **2008**, *112*, 12868-12886; c) M. Nayebzadeh, M. Vahedpour, A. Shiroudi, J. M. Rius-Bartra, *Chem. Phys.* **2020**, *528*, 110522; d) F. Shahsavar, E. Zahedi, A. Shiroudi, B. Chahkandi, *J. Mol. Graph. Model.* **2023**, *121*, 108426; e) A. Shiroudi, M. A. Abdel-Rahman, A. M. El-Nahas, M. Altarawneh, *New J. Chem.* **2021**, *45*, 2237-2248; f) J. Zheng, Y. Zhao, D. G. Truhlar, *J. Phys. Chem. A* **2007**, *111*, 4632-4642.

[56] S. Kanchanakungwankul, J. Bao, J. Zheng, I. Alecu, B. Lynch, Y. Zhao, D. Truhlar, *Database of Frequency Scale Factors for Electronic Model Chemistries-Version 4*, **2021**.
[57] a) K. Burke, J. Werschnik, E. Gross, *J Chem. Phys.* **2005**, *123*; b) G.-J. Zhao, K.-L. Han, *J. Phys. Chem. A* **2009**, *113*, 4788-4794; c) G.-J. Zhao, K.-L. Han, *Phys. Chem. Chem. Phys.* **2010**, *12*, 8914-8918; d) G.-J. Zhao, K.-L. Han, *Acc. Chem. Res.* **2012**, *45*, 404-413; e) S. Wang, Z. Wang, C. Hao, W. J. Peijnenburg, *Chemosphere* **2019**, *220*, 40-46.
[58] R. O. Ramabhadran, K. Raghavachari, *J. Chem. Theory Comput.* **2013**, *9*, 3986-3994.
[59] G. P. Wood, L. Radom, G. A. Petersson, E. C. Barnes, M. J. Frisch, J. A. Montgomery Jr, *J Chem. Phys.* **2006**, *125*, 094106.
[60] T. J. Lee, P. R. Taylor, *Int. J. Quantum Chem.* **1989**, *36*, 199-207.
[61] F. Jensen, *Introduction to Computational Chemistry*, John Wiley & Sons, **2017**.
[62] P. R. Taylor, *Lecture Notes in Quantum Chemistry II: European Summer School in Quantum Chemistry* **1994**, 125-202.
[63] a) C. Gonzalez, H. B. Schlegel, *J. Phys. Chem.* **1990**, *94*, 5523-5527; b) C. Gonzalez, H. B. Schlegel, *J. Chem. Phys.* **1989**, *90*, 2154-2161.
[64] a) H. Hratchian, H. Schlegel, *J. Chem. Theory Comput.* **2005**, *1*, 61-69; b) H. P. Hratchian, H. B. Schlegel, *J. Chem. Phys.* **2004**, *120*, 9918-9924; c) H. P. Hratchian, H. B. Schlegel, in *Theory and Applications of Computational Chemistry*, Elsevier, **2005**, pp. 195-249.
[65] a) R. G. Gilbert, S. C. Smith, *Theory of Unimolecular and Recombination Reactions*, Blackwell Scientific Publications, Oxford, UK, **1990**; b) H.-B. Rao, X.-Y. Zeng, H. He, Z.-R. Li, *The J. Phys. Chem. A* **2011**, *115*, 1602-1608; c) D. Varma, P. Raghunath, M.-C. Lin, *J. Phys. Chem. A* **2010**, *114*, 3642-3648; d) S. Wu, P. Raghunath, J.-S. Wu, M.-C. Lin, *J. Phys. Chem. A* **2010**, *114*, 633-639.
[66] a) E. Dzib, J. L. Cabellos, F. Ortíz-Chi, S. Pan, A. Galano, G. Merino, *Int. J. Quantum Chem.* **2019**, *119*, e25686; b) A. Quintal, E. Dzib, F. Ortíz-Chi, P. Jaque, A. Restrepo, G. Merino, *Int. J. Quantum Chem.* **2021**, *121*, e26684.
[67] a) C. Eckart, *Physical Review* **1930**, *35*, 1303; b) H. S. Johnston, J. Heicklen, *J. Phys. Chem.* **1962**, *66*, 532-533.

Table of Contents (ToC)

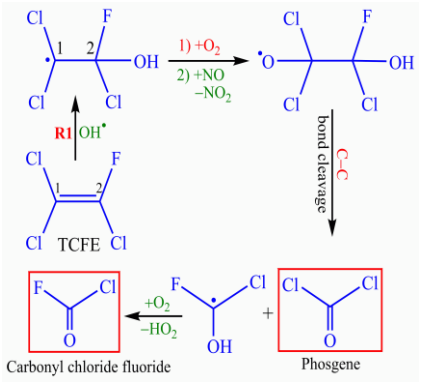

The degradation of Trichlorofluoroethene by OH• was analyzed using the M06-2X and CCSD(T) methods. The dominant pathway is OH addition to the C2 position (which is bonded to F and Cl) with an atmospheric lifetime of 8.49 days and negligible greenhouse gas emissions. Secondary reactions result in peroxy species and alkoxy radical, forming $COCl_2$ and CClFO, with phosgene as the primary product.

Chemical Investigation on the Mechanism and Kinetics of the Atmospheric Degradation Reaction of Trichlorofluoroethene by $OH^{\bullet}$ and Its Subsequent Fate in the Presence of O_2/NOx

Abolfazl Shiroudi,*[a,b] Jacek Czub,[a,b] and Mohammednoor Altarawneh[c]

[a] *Department of Physical Chemistry, Gdańsk University of Technology, Narutowicza 11/12, Gdańsk 80-233, Poland*

[b] *BioTechMed Center, Gdańsk University of Technology, Gdańsk 80-233, Poland*

[c] *United Arab Emirates University, Department of Chemical and Petroleum Engineering, Sheikh Khalifa bin Zayed Street, Al-Ain 15551, United Arab Emirates*

Supporting Information

Table S1. Cartesian coordinates of reactants, pre-reactive complexes, transition states, post-reactive complexes, and products optimized at the M06-2X/6-311++G(d,p) level of theory.

TCFE

0 1

C	-0.45428300	-0.73268200	0.00000000
C	0.00000000	0.51780100	0.00000000
F	-1.75101900	-0.98674700	0.00000000
Cl	0.51116500	-2.13825100	0.00000000
Cl	1.67168100	0.89464300	0.00000000
Cl	-1.09550100	1.84184400	0.00000000

Sum of electronic and zero-point Energies=	-1556.569142
Sum of electronic and thermal Energies=	-1556.563031
Sum of electronic and thermal Enthalpies=	-1556.562087
Sum of electronic and thermal Free Energies=	-1556.600850

OH radical

0 2

O	0.00000000	0.00000000	0.10802000
H	0.00000000	0.00000000	-0.86415900

Sum of electronic and zero-point Energies=	-75.717966
Sum of electronic and thermal Energies=	-75.715606
Sum of electronic and thermal Enthalpies=	-75.714662
Sum of electronic and thermal Free Energies=	-75.734888

* Corresponding author:
E-mail: abolfazl.shiroudi@pg.edu.pl (A. Shiroudi)

pre-RC1 species

0 2

C	-0.64366100	-0.44898800	-0.38705200
C	0.52495700	0.18128400	-0.24944800
F	-0.68513200	-1.74571500	-0.63200800
Cl	-2.17439400	0.27900000	-0.28189400
O	-0.22098400	-0.73339100	2.20978400
H	0.58415900	-1.27622500	2.14660000
Cl	0.64730700	1.85805700	0.05713100
Cl	2.00133100	-0.69817400	-0.38216700

Sum of electronic and zero-point Energies= -1632.292725
Sum of electronic and thermal Energies= -1632.283367
Sum of electronic and thermal Enthalpies= -1632.282423
Sum of electronic and thermal Free Energies= -1632.329517

pre-RC2 species

0 2

C	-0.68341800	-0.52779900	-0.29558900
C	0.48085300	0.13613800	-0.25263700
F	-0.69811800	-1.84642700	-0.39128900
O	0.20596600	-0.22385900	2.27390700
H	0.58715100	-1.12525200	2.24021200
Cl	0.57531700	1.83907600	-0.16925500
Cl	1.96065600	-0.73054500	-0.42521600
Cl	-2.22635100	0.17875900	-0.20673600

Sum of electronic and zero-point Energies= -1632.291302
Sum of electronic and thermal Energies= -1632.282356
Sum of electronic and thermal Enthalpies= -1632.281412
Sum of electronic and thermal Free Energies= -1632.327491

pre-RC3 species

0 2

C	0.94366500	0.52367500	0.04597900
C	-0.27289600	0.16149200	-0.35886100
Cl	-1.55033900	1.31432900	-0.38499300
Cl	-0.65603200	-1.43574700	-0.85295700
O	-1.72874400	-1.06643000	1.92294200
H	-2.54655100	-0.80186300	1.45321900
F	1.19181800	1.76515100	0.42252200
Cl	2.30199100	-0.50588000	0.13429300

Sum of electronic and zero-point Energies= -1632.287685
Sum of electronic and thermal Energies= -1632.279368
Sum of electronic and thermal Enthalpies= -1632.278424
Sum of electronic and thermal Free Energies= -1632.322958

pre-RC4 species

0 2

C	0.91550800	-0.54962900	-0.03130000
C	-0.24434600	0.00148900	-0.38655200
F	1.03260500	-1.85783400	0.10499500
Cl	-0.45601300	1.69287500	-0.57532600
Cl	-1.62068700	-0.99471700	-0.66108600
O	-1.94469100	0.26343700	2.02658100
H	-2.56341900	0.83898200	1.53172300
Cl	2.35908400	0.30554000	0.28451700

Sum of electronic and zero-point Energies= -1632.290340
Sum of electronic and thermal Energies= -1632.281830
Sum of electronic and thermal Enthalpies= -1632.280886
Sum of electronic and thermal Free Energies= -1632.326317

pre-RC5 species

0 2

C	-0.83674800	0.04597300	-0.04476900
C	0.36278800	-0.34569300	-0.49460600
Cl	1.67387000	0.74619000	-0.76109000
O	2.91958300	-0.63512200	1.54648800
Cl	-1.28408500	1.66198800	0.33581000
H	3.77204300	-0.21956500	1.39740800
F	0.59486700	-1.64935200	-0.75749600
Cl	-2.13324100	-1.11741100	0.20671600

Sum of electronic and zero-point Energies= -1632.287078
Sum of electronic and thermal Energies= -1632.278483
Sum of electronic and thermal Enthalpies= -1632.277538
Sum of electronic and thermal Free Energies= -1632.324877

TS1 (related to the OH attack onto C_2)

0 2

C	-0.62399500	-0.45928500	-0.24488900
C	0.58267100	0.15751700	-0.17238800
F	-0.68346500	-1.74137500	-0.54193100
Cl	-2.11162200	0.35196800	-0.37228200
O	-0.59720200	-0.66021600	1.87731400
H	0.11517500	-1.30860100	2.00049500
Cl	0.74042000	1.83274400	0.07263200
Cl	2.02188100	-0.76863500	-0.26729000

Sum of electronic and zero-point Energies= -1632.288687
Sum of electronic and thermal Energies= -1632.280548
Sum of electronic and thermal Enthalpies= -1632.279604
Sum of electronic and thermal Free Energies= -1632.323331

TS2 (related to the OH attack onto C_1)

0 2

C	-0.70332400	-0.55566500	-0.21193000
C	0.48431400	0.10323000	-0.10358200
F	-0.72326600	-1.87143200	-0.25480300
O	0.29654300	0.00682700	1.95830500
H	0.59886500	-0.90080200	2.12169800
Cl	0.56872700	1.80425400	-0.24667700
Cl	1.94570800	-0.76985200	-0.37698400
Cl	-2.22901000	0.16581500	-0.17644700

Sum of electronic and zero-point Energies= -1632.285337
Sum of electronic and thermal Energies= -1632.277256
Sum of electronic and thermal Enthalpies= -1632.276312
Sum of electronic and thermal Free Energies= -1632.319851

TS3 (related to the removal of chlorine atom bonded to the C_1 in *cis* mode)

0 2

C	-1.25762800	-0.51597200	0.00201800
C	-0.51968900	0.57153000	-0.00002000
F	-2.58694400	-0.47171900	-0.01109200
O	3.39498500	-0.31786600	0.12969000
H	3.43020500	-0.99409600	-0.55956000
Cl	-0.95396000	2.18460200	0.01325800
Cl	1.79634700	0.36695100	-0.04886500
Cl	-0.64495700	-2.11336900	0.01265900

Sum of electronic and zero-point Energies= -1632.223318
Sum of electronic and thermal Energies= -1632.215203
Sum of electronic and thermal Enthalpies= -1632.214259
Sum of electronic and thermal Free Energies= -1632.259495

TS4 (related to the removal of chlorine atom bonded to the C_1 in *trans* mode)

0 2

C	1.09293900	-0.64429400	-0.05961500
C	0.34528600	0.43657100	-0.06403800
F	0.57337800	-1.87063000	-0.13450700
Cl	0.63554600	2.07734300	-0.05969100
Cl	-2.21854300	-0.02594800	0.17521800
O	-3.87957900	-0.50655600	-0.15225600
H	-3.84790200	-1.46934800	-0.05071400
Cl	2.82386700	-0.66293600	0.07395700

Sum of electronic and zero-point Energies= -1632.229526
Sum of electronic and thermal Energies= -1632.221200
Sum of electronic and thermal Enthalpies= -1632.220256
Sum of electronic and thermal Free Energies= -1632.267628

TS5 (related to the removal of chlorine atom bonded to the C_2)

0 2

C	1.22515800	0.07995700	0.03432300
C	0.20840600	-0.76631100	0.05618600
Cl	-2.33477000	0.00551100	-0.21071000
O	-4.04301900	-0.01702600	0.13401800
H	-4.10036200	0.52303900	0.94503400
Cl	2.87828700	-0.48619900	-0.02682800
F	0.21366800	-2.06928500	0.08883300
Cl	0.98119600	1.79568000	0.03990700

Sum of electronic and zero-point Energies= -1632.221012
Sum of electronic and thermal Energies= -1632.213297
Sum of electronic and thermal Enthalpies= -1632.212353
Sum of electronic and thermal Free Energies= -1632.258974

IM2 (OH attack onto C_2 position)

0 2

C	0.77917000	0.04413500	-0.45637400
C	-0.70659600	0.01443800	-0.29217500
F	1.18345100	-1.06636000	-1.12089800
Cl	1.60658900	-0.05048100	1.17362600
O	1.14519200	1.16571100	-1.11046200
H	2.10614900	1.25166000	-1.08637200
Cl	-1.48931600	1.44497700	0.17908600
Cl	-1.43222500	-1.47282300	0.09137200

Sum of electronic and zero-point Energies= -1632.366888
Sum of electronic and thermal Energies= -1632.359298
Sum of electronic and thermal Enthalpies= -1632.358354
Sum of electronic and thermal Free Energies= -1632.401245

pre-reactive complex IM3b [TCFE-OH…O_2]$^{\bullet}$

0 2

C	0.83757200	-0.64915000	-0.01683000
C	-0.17311300	0.45042900	-0.02906400
F	0.71760900	-1.35894900	1.13205300
Cl	2.53441200	0.03876600	0.02371800
O	0.66999000	-1.43718100	-1.09849100
H	1.40816800	-2.05539900	-1.16208300
Cl	-0.51598800	1.22466800	-1.49904100
Cl	-0.46292800	1.29027400	1.41765900
O	-2.22081200	-1.33743700	0.06704200
O	-3.23628300	-0.71723000	0.06010500

Sum of electronic and zero-point Energies= -1782.676086
Sum of electronic and thermal Energies= -1782.665294
Sum of electronic and thermal Enthalpies= -1782.664350
Sum of electronic and thermal Free Energies= -1782.716734

TS2 [TCFE-OH…O_2]•

0 2

C	0.81480300	-0.53759500	-0.31802100
C	-0.32396000	0.37752100	0.05949000
F	0.56680400	-1.77460200	0.17774900
Cl	2.36179700	0.00323600	0.47059600
O	0.93451100	-0.56534800	-1.65976100
H	1.71148700	-1.08328800	-1.90344000
Cl	-0.36470200	1.90262300	-0.70118000
Cl	-0.88416300	0.27611100	1.65730900
O	-1.84740900	-0.69412600	-0.95099400
O	-2.67180500	-1.12531600	-0.18917500

Sum of electronic and zero-point Energies= -1782.672200
Sum of electronic and thermal Energies= -1782.662187
Sum of electronic and thermal Enthalpies= -1782.661243
Sum of electronic and thermal Free Energies= -1782.709850

IM3 [TCFE-OH–O_2]•

0 2

C	0.92583000	-0.23902100	0.53641000
C	-0.51399000	-0.00449000	-0.00975500
F	1.08758900	0.55178500	1.62382100
Cl	2.15920400	0.26637700	-0.65545200
O	1.03404000	-1.54011100	0.86538100
H	1.92044900	-1.71720600	1.20400500
Cl	-0.83081600	-1.00734400	-1.41754400
Cl	-0.79025700	1.69808000	-0.35495600
O	-1.34113600	-0.41521900	1.08488800
O	-2.60890500	-0.30201000	0.83683900

Sum of electronic and zero-point Energies= -1782.703900
Sum of electronic and thermal Energies= -1782.694526
Sum of electronic and thermal Enthalpies= -1782.693582
Sum of electronic and thermal Free Energies= -1782.739994

TS3 [TCFE-OH–OO…NO]• (with removal of NO_2)

0 1

C	0.09731500	0.33986300	-0.12132300
C	1.59788800	-0.14403000	-0.16531000
Cl	-0.61541500	-0.19254900	1.54068100
F	2.22046500	0.23723200	0.97461200
O	2.24181200	0.34423600	-1.24927800
H	2.08681900	1.29945200	-1.28813800
O	-0.59452200	-0.03459200	-1.10271100
O	-3.08506400	-1.45245400	-0.13159000
N	-3.06584000	-0.33854700	-0.36394500
O	-2.55125800	0.61189600	-0.69031900
Cl	0.21621100	2.22422800	0.01674700
Cl	1.64219900	-1.91358300	-0.25300200

Sum of electronic and zero-point Energies= -1912.582393
Sum of electronic and thermal Energies= -1912.570514
Sum of electronic and thermal Enthalpies= -1912.569570
Sum of electronic and thermal Free Energies= -1912.622254

pre-reactive complex IM4b [TCFE-OH-O_2-NO]

0 1

C	0.08582800	0.46985000	0.04769500
C	1.41927000	-0.30955400	-0.22462900
Cl	-0.49838000	0.19605300	1.69548200
F	2.30171100	0.09540300	0.72067200
O	1.90421900	-0.08384900	-1.46569800
H	1.99878800	0.87002600	-1.59939200
O	-0.79051600	0.01504200	-0.91456300
O	-2.66124200	-1.39073500	-0.15728300
N	-3.05815800	-0.33509300	-0.34146900
O	-2.03992700	0.63246200	-0.77130400
Cl	0.41610500	2.21996500	-0.17513000
Cl	1.16239600	-2.04708500	-0.04764500

Sum of electronic and zero-point Energies= -1912.617099
Sum of electronic and thermal Energies= -1912.605732
Sum of electronic and thermal Enthalpies= -1912.604788
Sum of electronic and thermal Free Energies= -1912.655420

IM4 [TCFE-OH–O]•

0 2

C	0.68395500	0.02663000	0.33494000
C	-0.87291900	-0.03797400	0.43325900
Cl	1.30401700	-1.37567500	-0.58925800
F	-1.20258300	-1.23785600	0.96371400
O	-1.24981900	0.96653700	1.25055500
H	-2.20819000	0.95293500	1.36465300
O	1.24273200	-0.17786500	1.52868700
Cl	-1.65856900	0.04603400	-1.17051700
Cl	1.19113600	1.56178600	-0.40970700

Sum of electronic and zero-point Energies= -1707.560846
Sum of electronic and thermal Energies= -1707.552479
Sum of electronic and thermal Enthalpies= -1707.551535
Sum of electronic and thermal Free Energies= -1707.595512

TS4a [TCFE-OH–O]• (with removal of •Cl)

0 2

C	0.61253500	0.26901000	0.46796500
C	-0.91984700	-0.03907400	0.42886900
Cl	1.48168200	-1.41129500	-0.44309000
F	-1.12649700	-1.20622000	1.07053600
O	-1.49635600	0.98820800	1.09139500
H	-2.45559200	0.87747100	1.09519700
O	1.23175500	0.02373500	1.50964200
Cl	-1.56192500	-0.22590000	-1.22583700
Cl	1.05405200	1.66680300	-0.50279800

Sum of electronic and zero-point Energies= -1707.553935
Sum of electronic and thermal Energies= -1707.545639
Sum of electronic and thermal Enthalpies= -1707.544695
Sum of electronic and thermal Free Energies= -1707.588807

IM5a (2-chloro-2-fluro-2hydroxyacetyl chloride)

0 1

C	-0.76133800	0.58262600	-0.23540200
C	0.64889900	0.26209200	0.31245000
F	1.41727900	1.35606200	0.14884100
O	0.55972300	-0.09095000	1.60822900
H	1.43114400	-0.34310100	1.93962200
Cl	1.36487700	-1.03104000	-0.71121100
Cl	-1.95082800	-0.65176200	0.13651100
O	-1.00358100	1.55068400	-0.85467700

Sum of electronic and zero-point Energies= -1247.441615
Sum of electronic and thermal Energies= -1247.434542
Sum of electronic and thermal Enthalpies= -1247.433597
Sum of electronic and thermal Free Energies= -1247.474323

TS4b [TCFE-OH–O]$^{\bullet}$ (with cleavage of the C–C bond)

0 2

C	0.78204300	0.03611500	0.45626000
C	-0.99857100	0.07523400	0.40524200
Cl	1.30644400	-1.51111300	-0.27606300
F	-1.38326300	-0.89693400	1.20496000
O	-1.42394200	1.23771500	0.88324500
H	-1.09874600	1.96469800	0.33355900
O	1.00147700	0.19184500	1.66716000
Cl	-1.50289600	-0.26350900	-1.25561000
Cl	1.26862700	1.42186500	-0.63011800

Sum of electronic and zero-point Energies= -1707.559769
Sum of electronic and thermal Energies= -1707.551520
Sum of electronic and thermal Enthalpies= -1707.550576
Sum of electronic and thermal Free Energies= -1707.594406

pre-reactive complex IM5b | [C(OH)ClF…O_2]$^{\bullet}$

0 2

C	0.54592200	0.53574100	0.18498800
O	-0.11265200	0.80940500	1.12162900
F	0.58968300	1.26102400	-0.90823400
H	-1.97930000	0.22571900	0.86472000
O	-2.49635700	-0.30577400	0.22252900
O	-1.66237800	-0.65236200	-0.71426600
Cl	1.62163000	-0.79997200	0.06825400

Sum of electronic and zero-point Energies= -824.231714
Sum of electronic and thermal Energies= -824.224389
Sum of electronic and thermal Enthalpies= -824.223445
Sum of electronic and thermal Free Energies= -824.265893

IM5 [•C(OH)ClF]

0 2

C	-0.40816800	0.00610400	0.32433200
O	-1.05703100	-1.08693600	-0.09667800
F	-0.99042900	1.14572700	-0.08015400
H	-2.00310700	-0.96077900	0.04824500
Cl	1.28366000	-0.04070000	-0.02937800

Sum of electronic and zero-point Energies= -673.870778
Sum of electronic and thermal Energies= -673.866558
Sum of electronic and thermal Enthalpies= -673.865613
Sum of electronic and thermal Free Energies= -673.898814

TS5 [C(OH)ClF…O_2]• (with removal of HO_2 radical)

0 2

C	0.14243600	0.40282700	0.15674300
O	-0.46681100	0.51566700	1.23066500
F	0.29206300	1.46500800	-0.62329400
H	-1.51962200	-0.08224300	0.91098900
O	-2.01360100	-0.63490200	-0.00151100
O	-1.05010100	-0.47648800	-0.81142600
Cl	1.54591500	-0.63258800	0.02449300

Sum of electronic and zero-point Energies= -824.215972
Sum of electronic and thermal Energies= -824.210634
Sum of electronic and thermal Enthalpies= -824.209690
Sum of electronic and thermal Free Energies= -824.246413

$COCl_2$ | Carbonyl chloride (phosgene)

0 1

C	0.00000000	0.00000000	0.49302500
O	0.00000000	0.00000000	1.66239500
Cl	0.00000000	1.45190300	-0.47815600
Cl	0.00000000	-1.45190300	-0.47815600

Sum of electronic and zero-point Energies= -1033.697426
Sum of electronic and thermal Energies= -1033.693534
Sum of electronic and thermal Enthalpies= -1033.692590
Sum of electronic and thermal Free Energies= -1033.724663

Carbonyl chloride fluoride | CClFO

0 1

C	0.00000000	0.50572900	0.00000000
O	-0.80306500	1.35360100	0.00000000
Cl	-0.31226700	-1.19587200	0.00000000
F	1.30367300	0.71851600	0.00000000

Sum of electronic and zero-point Energies= -673.346157
Sum of electronic and thermal Energies= -673.342591
Sum of electronic and thermal Enthalpies= -673.341647
Sum of electronic and thermal Free Energies= -673.373010

IM6 [TCFE-OH]$^{\bullet}$ (OH attack onto C_1 position)

0 2

C	-0.77120500	-0.65547400	-0.06305500
C	0.45054400	0.10547400	0.34736000
F	-0.68647100	-1.24533100	-1.23961900
O	0.28257600	0.54114500	1.61642700
H	1.02595200	1.10267600	1.86728800
Cl	0.71114000	1.51047100	-0.78845200
Cl	1.87297800	-0.98408400	0.19177800
Cl	-2.30084500	0.00750400	0.28208800

Sum of electronic and zero-point Energies= -1632.353988
Sum of electronic and thermal Energies= -1632.346368
Sum of electronic and thermal Enthalpies= -1632.345424
Sum of electronic and thermal Free Energies= -1632.388159

IM7b [TCFE-OH–O_2]$^{\bullet}$

0 2

C	0.77622900	0.00606300	0.34895500
C	-0.67748500	0.02932900	-0.19634000
Cl	1.66356500	-1.34410800	-0.42571100
O	0.69735300	-0.13099800	1.68978500
H	1.58107400	-0.11155400	2.07708500
Cl	-1.56220200	-1.43322000	0.20946800
O	-1.28836000	1.16283200	0.40905100
O	-2.49214100	1.36421000	-0.04196400
Cl	1.57839700	1.53995900	-0.12483600
F	-0.67380700	0.19623600	-1.51660100

Sum of electronic and zero-point Energies= -1782.702466
Sum of electronic and thermal Energies= -1782.693129
Sum of electronic and thermal Enthalpies= -1782.692185
Sum of electronic and thermal Free Energies= -1782.738577

pre-reactive complex-IM7b [TCFE-OH…O_2]$^{\bullet}$

0 2

C	-0.78042900	-0.29158800	0.34844400
C	0.29853600	0.61964300	-0.14683000
Cl	-2.29105000	-0.06975700	-0.65871200
O	-1.02352700	-0.00660200	1.64759700
H	-1.76342100	-0.55187000	1.96159900
Cl	0.20716100	2.28145900	0.22889800
O	2.64135900	-0.30859400	0.59473500
O	3.07599700	-0.72673600	-0.44124100
Cl	-0.23185800	-1.99255300	0.11992600
F	0.71909600	0.35482800	-1.36799000

Sum of electronic and zero-point Energies= -1782.700262
Sum of electronic and thermal Energies= -1782.690884
Sum of electronic and thermal Enthalpies= -1782.689939
Sum of electronic and thermal Free Energies= -1782.736416

NO_2

0 2

O	1.09057400	-0.13801200	0.00000000
N	0.00000000	0.31546300	0.00000000
O	-1.09057400	-0.13801800	0.00000000

Sum of electronic and zero-point Energies= -205.041489
Sum of electronic and thermal Energies= -205.038566
Sum of electronic and thermal Enthalpies= -205.037622
Sum of electronic and thermal Free Energies= -205.065459

TS7b [TCFE-OH…O_2]$^{\bullet}$

0 2

C	-0.73432200	-0.20928200	0.33721400
C	0.46221300	0.49262900	-0.23675100
Cl	-2.24853700	0.43202200	-0.44987400
O	-0.74894900	0.01199700	1.67066800
H	-1.53740600	-0.38655600	2.05868900
Cl	0.71385900	2.12515500	0.17452700
O	2.14489700	-0.55629100	0.62476900
O	2.75189400	-1.11506900	-0.24767500
Cl	-0.62222100	-1.95727900	-0.05852300
F	0.73940000	0.19590200	-1.48530800

Sum of electronic and zero-point Energies= -1782.660006
Sum of electronic and thermal Energies= -1782.649825
Sum of electronic and thermal Enthalpies= -1782.648881
Sum of electronic and thermal Free Energies= -1782.698044

pre-reactive complex IM8b [TCFE-OH-O_2…NO]

0 1

C	-0.08769800	-0.54754800	0.24101800
C	1.21334700	0.31435000	0.36847700
Cl	-0.52051500	-0.95123400	-1.42118000
O	1.48904900	0.54131500	1.68159700
H	1.58344700	-0.30745200	2.13561600
O	-1.06247500	0.17750600	0.89124600
O	-2.89513000	1.09848000	-0.45793900
N	-3.27342300	0.15207500	0.06116500
O	-2.27288800	-0.53258000	0.88044300
Cl	0.98584600	1.87494400	-0.41690600
Cl	2.55259000	-0.58944800	-0.42120500
F	0.13372300	-1.70201300	0.91382400

Sum of electronic and zero-point Energies= -1912.614779
Sum of electronic and thermal Energies= -1912.603397
Sum of electronic and thermal Enthalpies= -1912.602453
Sum of electronic and thermal Free Energies= -1912.653297

IM8 [TCFE-OH–O]•

0 2

C	0.71431400	-0.54643700	-0.23293800
C	-0.56164400	0.12485800	0.35430100
O	-0.40336400	0.20764900	1.69090800
H	-1.18892500	0.59760400	2.09276200
O	0.93483000	-1.74572900	0.29005100
Cl	-0.81231400	1.72642700	-0.39954400
Cl	2.19560000	0.34964300	0.22286400
F	0.61777700	-0.56172900	-1.57536700
Cl	-1.94439300	-0.94124300	-0.08745500

Sum of electronic and zero-point Energies= -1707.560978
Sum of electronic and thermal Energies= -1707.552617
Sum of electronic and thermal Enthalpies= -1707.551673
Sum of electronic and thermal Free Energies= -1707.595720

NO

0 2

O	0.00000000	0.00000000	0.53124000
N	0.00000000	0.00000000	-0.60713100

Sum of electronic and zero-point Energies= -129.875527
Sum of electronic and thermal Energies= -129.873166
Sum of electronic and thermal Enthalpies= -129.872222
Sum of electronic and thermal Free Energies= -129.895499

TS8 [TCFE-OH–OO…NO]•

0 1

C	-0.04754600	-0.48447700	0.41592100
C	1.35983100	0.23380400	0.37242500
Cl	-0.67051500	-0.70432400	-1.37138600
O	1.87271200	0.26731300	1.63431700
H	1.84069400	-0.62962500	1.99440400
O	-0.88443600	0.10712000	1.15206800
O	-3.14803100	1.17126300	-0.49010700
N	-3.21356800	0.18637700	0.07186100
O	-2.82079500	-0.63909900	0.72838600
Cl	1.15795800	1.90387600	-0.17156500
F	0.22844500	-1.78684100	0.81404100
Cl	2.48720200	-0.63144400	-0.73653000

Sum of electronic and zero-point Energies= -1912.578166
Sum of electronic and thermal Energies= -1912.566324
Sum of electronic and thermal Enthalpies= -1912.565380
Sum of electronic and thermal Free Energies= -1912.618341

IM9c [$C(OH)Cl_2$–C(O)F] (with removal Cl•)

0 1

C	-1.27485100	-0.00091900	-0.02165100
C	0.20772500	0.00042900	0.37328500
O	0.27096100	0.00105300	1.71833900
H	1.19343500	0.00403200	2.00201200
O	-2.18147200	-0.00043400	0.71992500
Cl	0.97853400	-1.46047100	-0.33828900
F	-1.41412100	-0.00261200	-1.34267800
Cl	0.97561300	1.46149800	-0.34017200

Sum of electronic and zero-point Energies= -1247.439742
Sum of electronic and thermal Energies= -1247.432627
Sum of electronic and thermal Enthalpies= -1247.431683
Sum of electronic and thermal Free Energies= -1247.472349

HO_2

0 2

O	0.05493600	0.70821000	0.00000000
O	0.05493600	-0.59909800	0.00000000
H	-0.87898300	-0.87289900	0.00000000

Sum of electronic and zero-point Energies= -150.875982
Sum of electronic and thermal Energies= -150.873130
Sum of electronic and thermal Enthalpies= -150.872186
Sum of electronic and thermal Free Energies= -150.898123

IM9a [C(OH)Cl_2–C(O)Cl] (with removal $F^{\bullet}$)

0 1

C	0.90598400	-0.09840000	0.67551800
C	-0.60783100	-0.04720400	0.33560800
O	-1.27160500	-0.21139500	1.49714400
H	-2.22262700	-0.18712900	1.33499400
O	1.30730100	-0.25845300	1.76642700
Cl	-0.97956600	1.53684600	-0.42530300
Cl	-0.98240800	-1.35612400	-0.83626900
Cl	1.97068700	0.10278000	-0.70962400

Sum of electronic and zero-point Energies= -1607.790531
Sum of electronic and thermal Energies= -1607.783069
Sum of electronic and thermal Enthalpies= -1607.782125
Sum of electronic and thermal Free Energies= -1607.824035

IM9=IM9b [C(OH)Cl_2–C(O)ClF]$^{\bullet}$ (with removal of CClFO)

0 2

C	-0.01539000	0.35403600	0.31680800
O	-0.05126200	1.62330000	-0.11273500
H	0.78006100	2.05912200	0.11114100
Cl	-1.48009600	-0.48405100	-0.03039800
Cl	1.46376500	-0.52593400	-0.03490300

Sum of electronic and zero-point Energies= -1034.226728
Sum of electronic and thermal Energies= -1034.222233
Sum of electronic and thermal Enthalpies= -1034.221289
Sum of electronic and thermal Free Energies= -1034.255726

TS9a species (with removal of chlorine atom)

0 2

C	0.56612700	-0.71222700	-0.25833700
C	-0.58963600	0.12112800	0.35170900
O	-0.38220800	0.20312100	1.67905000
H	-1.11243600	0.67537800	2.09719800
O	0.99724900	-1.71391800	0.31862000
Cl	-0.71613200	1.72286700	-0.42730600
Cl	2.30652400	0.33501300	0.20524900
F	0.52307500	-0.68143600	-1.58453000
Cl	-2.08301000	-0.81726200	-0.03547300

Sum of electronic and zero-point Energies= -1707.554914
Sum of electronic and thermal Energies= -1707.546586
Sum of electronic and thermal Enthalpies= -1707.545641
Sum of electronic and thermal Free Energies= -1707.589830

TS9c species (with removal of fluorine atom)

0	2		
C	-0.74378600	-0.59581100	-0.18122100
C	0.57081500	0.22592000	-0.37474600
O	0.50720600	0.64639800	-1.66555800
H	1.29557300	1.15923100	-1.88376000
O	-0.78617000	-1.80131600	-0.33535400
Cl	0.64782100	1.59947100	0.76699400
Cl	-2.18765800	0.36882200	-0.28976600
F	-0.59399500	-0.99017700	1.62475800
Cl	1.97042000	-0.83823100	-0.08875600

Sum of electronic and zero-point Energies= -1707.503968
Sum of electronic and thermal Energies= -1707.495393
Sum of electronic and thermal Enthalpies= -1707.494448
Sum of electronic and thermal Free Energies= -1707.539088

IM9 [$^{\bullet}C(OH)Cl_2$]

0	2		
C	-0.01539000	0.35403600	0.31680800
O	-0.05126200	1.62330000	-0.11273500
H	0.78006100	2.05912200	0.11114100
Cl	-1.48009600	-0.48405100	-0.03039800
Cl	1.46376500	-0.52593400	-0.03490300

Sum of electronic and zero-point Energies= -1034.226728
Sum of electronic and thermal Energies= -1034.222233
Sum of electronic and thermal Enthalpies= -1034.221289
Sum of electronic and thermal Free Energies= -1034.255726

pre-reactive complex IM10 [TCFE-OH-O_2…NO]

0	2		
C	0.48868700	0.00027200	0.48600400
O	-0.25353100	-0.00832200	1.40208200
H	-2.15282600	-0.00960300	0.88284700
O	-2.69905000	-0.01077400	0.06869100
O	-1.86218500	-0.01170200	-0.92862400
Cl	1.09518900	1.45576100	-0.23765400
Cl	1.12474200	-1.44079900	-0.24093900

Sum of electronic and zero-point Energies= -1184.582809
Sum of electronic and thermal Energies= -1184.575036
Sum of electronic and thermal Enthalpies= -1184.574092
Sum of electronic and thermal Free Energies= -1184.618430

TS10 [$^{\bullet}$C(OH)Cl_2…O_2] (with removal of HO_2 radical)

0 2

C	-0.26318200	0.20702800	0.00000000
O	-1.47148900	-0.09006300	0.00000000
H	-1.37756800	-1.31484500	0.00000000
O	-0.56045900	-2.18511200	0.00000000
O	0.45743400	-1.43414100	0.00000000
Cl	0.45743400	0.87491800	1.45752600
Cl	0.45743400	0.87491800	-1.45752600

Sum of electronic and zero-point Energies= -1184.564639
Sum of electronic and thermal Energies= -1184.558849
Sum of electronic and thermal Enthalpies= -1184.557905
Sum of electronic and thermal Free Energies= -1184.596066

$^{\bullet}$CCl_2–C(O)Cl | (IM2 [TCFE–OH]$^{\bullet}$ → *via* 1,2-HF-loss → product)

0 2

C	0.65709700	-0.76992500	-0.00001400
C	-0.53118700	0.07209600	-0.00000400
O	0.62624900	-1.96013300	-0.00001600
Cl	-0.50047600	1.76205700	-0.00000700
Cl	-2.03795500	-0.69775300	0.00001000
Cl	2.19928600	0.10440400	0.00001100

Sum of electronic and zero-point Energies= -1531.938092
Sum of electronic and thermal Energies= -1531.931835
Sum of electronic and thermal Enthalpies= -1531.930891
Sum of electronic and thermal Free Energies= -1531.970945

$^{\bullet}$CCl_2–C(O)F | (IM2 [TCFE–OH]$^{\bullet}$ → *via* 1,2-HCl-loss → product)

0 2

C	-1.18106700	-0.32559100	0.00020400
C	0.23266100	0.01192100	0.00008700
O	-1.64251900	-1.41774700	-0.00002000
Cl	0.77891300	1.61250300	0.00000300
Cl	1.36290000	-1.24202000	-0.00006700
F	-1.95335800	0.76953300	-0.00005600

Sum of electronic and zero-point Energies= -1171.587037
Sum of electronic and thermal Energies= -1171.581129
Sum of electronic and thermal Enthalpies= -1171.580185
Sum of electronic and thermal Free Energies= -1171.618918

$CCl_2F–^{\bullet}C(OH)Cl$ | (IM2 [TCFE–OH]$^{\bullet}$ → *via* 1,2-F-migration → product)

0 2

C	-0.74268700	-0.58635800	-0.33017100
C	0.49370900	0.07552400	0.21703500
O	-0.75409600	-1.91400800	-0.15881600
H	-1.57882900	-2.28627900	-0.49087000
Cl	1.93016100	-0.82679800	-0.29348900
Cl	0.60184400	1.75723800	-0.32978400
Cl	-2.24562000	0.24088400	-0.06540200
F	0.47076900	0.08342700	1.57196500

Sum of electronic and zero-point Energies= -1632.353920
Sum of electronic and thermal Energies= -1632.346271
Sum of electronic and thermal Enthalpies= -1632.345327
Sum of electronic and thermal Free Energies= -1632.388301

$CCl_3–^{\bullet}C(OH)F$ | (IM2 [TCFE–OH]$^{\bullet}$ → *via* 1,2-Cl-migration → product)

0 2

C	1.16288100	-0.02012200	-0.56895600
C	-0.23531800	0.01329000	-0.02746200
O	1.89324800	1.06548000	-0.30971400
H	2.79790300	0.92924800	-0.61478500
Cl	-1.02954500	1.49545800	-0.58151400
Cl	-0.20299100	-0.01613400	1.77064100
Cl	-1.10608000	-1.41294100	-0.62080000
F	1.80524600	-1.17117600	-0.33228400

Sum of electronic and zero-point Energies= -1632.349527
Sum of electronic and thermal Energies= -1632.341824
Sum of electronic and thermal Enthalpies= -1632.340880
Sum of electronic and thermal Free Energies= -1632.383543

$CHCl_2–C(O^{\bullet})ClF$ | (IM2 [TCFE–OH]$^{\bullet}$ → *via* 1,3-H-migration → product)

0 2

C	-0.83356100	-0.00948600	-0.48770700
C	0.71374900	0.02598900	-0.56318200
F	-1.28494200	1.14319600	-1.03733800
Cl	-1.45882800	-0.11814400	1.18838800
O	-1.34661200	-1.08412500	-1.06371800
H	0.97624900	0.09643100	-1.61668400
Cl	1.41735800	-1.45476500	0.08277500
Cl	1.34029300	1.46636600	0.24459000

Sum of electronic and zero-point Energies= -1632.340818
Sum of electronic and thermal Energies= -1632.333588
Sum of electronic and thermal Enthalpies= -1632.332644
Sum of electronic and thermal Free Energies= -1632.374593

•CCl(O)CClF | (IM2 [TCFE–OH]• → *via* 1,3-HCl-loss with cyclization → product)

0 2

C	0.73961100	-0.71764700	-0.10599200
C	-0.66843600	-0.41509300	-0.06592000
Cl	2.10419500	0.30046100	-0.18900700
F	-1.55472400	-1.25591700	-0.58539000
O	0.02596200	-0.89931700	1.05236100
Cl	-1.31844400	1.18743500	0.06436500

Sum of electronic and zero-point Energies= -1171.517927
Sum of electronic and thermal Energies= -1171.512514
Sum of electronic and thermal Enthalpies= -1171.511570
Sum of electronic and thermal Free Energies= -1171.549003

CCl_2=C(OH)Cl | (IM2 [TCFE–OH]• → *via* F-atom loss → product)

0 1

C	0.64803300	-0.58361000	-0.00547700
C	-0.51520000	0.06920700	0.00838900
O	0.70412800	-1.92258100	-0.08539300
H	1.50629700	-2.24565400	0.33856800
Cl	-0.63858900	1.78268800	-0.01260000
Cl	-1.99842700	-0.80245500	0.01824900
Cl	2.17017400	0.23816300	0.01359200

Sum of electronic and zero-point Energies= -1532.545798
Sum of electronic and thermal Energies= -1532.539148
Sum of electronic and thermal Enthalpies= -1532.538204
Sum of electronic and thermal Free Energies= -1532.577869

CCl_2–C(OH)F | (IM2 [TCFE–OH]• → *via* Cl-atom loss → product)

0 2

C	-1.08561100	-0.03127700	-0.00275800
C	0.24229700	0.01569300	0.01070100
F	-1.73354100	-1.19306900	0.02494100
O	-1.88447300	1.03011200	-0.08549800
H	-2.72081200	0.84060400	0.35614900
Cl	1.07102700	1.52095700	0.01502100
Cl	1.19122800	-1.41803800	-0.01174400

Sum of electronic and zero-point Energies= -1172.188018
Sum of electronic and thermal Energies= -1172.181671
Sum of electronic and thermal Enthalpies= -1172.180726
Sum of electronic and thermal Free Energies= -1172.219289

TS | (IM2 [TCFE–OH]$^{\bullet}$ → *via* 1,2-HF-loss → TS)

0 2

C	0.63913600	0.17530900	-0.15244400
C	-0.66086400	-0.42443900	-0.25478900
Cl	0.86854300	1.79170300	0.26341500
F	-0.77692500	-1.18265600	1.51850000
O	-0.80058700	-1.64845100	-0.63119900
H	-0.86611500	-1.95631400	0.41111800
Cl	1.99289000	-0.81801600	-0.28874800
Cl	-2.01475600	0.63117200	-0.36199800

Sum of electronic and zero-point Energies= -1632.308238
Sum of electronic and thermal Energies= -1632.300646
Sum of electronic and thermal Enthalpies= -1632.299702
Sum of electronic and thermal Free Energies= -1632.342833

TS | (IM2 [TCFE–OH]$^{\bullet}$ → *via* 1,2-HCl-loss → TS)

0 2

C	0.56087200	-0.13214300	-0.14906000
C	-0.09271400	1.03953800	-0.56421100
Cl	1.87011600	-0.03409000	0.92089000
O	-1.21282200	1.07711900	-1.15111400
H	-1.80460700	0.41247700	-0.57421900
Cl	0.32068600	-1.58403500	-0.99539000
F	0.46980100	2.18110400	-0.29264600
Cl	-1.92785900	-0.38797700	1.05665100

Sum of electronic and zero-point Energies= -1632.338635
Sum of electronic and thermal Energies= -1632.331230
Sum of electronic and thermal Enthalpies= -1632.330285
Sum of electronic and thermal Free Energies= -1632.373143

TS | (IM2 [TCFE–OH]$^{\bullet}$ → *via* 1,2-F-migration → TS)

0 2

C	-0.66968100	-0.55322800	-0.22969200
C	0.53652600	0.11027000	-0.12271700
O	-0.68671600	-1.85689400	-0.40077900
H	-1.50683000	-2.23595200	-0.05984400
Cl	1.98932800	-0.76278700	-0.26866400
Cl	0.64024500	1.80675600	-0.14545800
Cl	-2.16252800	0.27360000	-0.22036300
F	-0.01558900	-0.29442400	1.79630800

Sum of electronic and zero-point Energies= -1632.303118
Sum of electronic and thermal Energies= -1632.295509
Sum of electronic and thermal Enthalpies= -1632.294565
Sum of electronic and thermal Free Energies= -1632.336953

TS | (IM2 [TCFE–OH]$^{\bullet}$ → *via* 1,2-Cl-migration → TS)

0 2

C	0.69281700	0.03574500	-0.77319300
C	-0.46256700	0.00652800	0.03641200
O	1.32822100	1.15369800	-1.07608200
H	2.25027300	0.95015400	-1.31711000
Cl	-1.40476700	1.47800300	0.04239600
Cl	-1.39959000	-1.46954700	-0.05726900
F	1.34960500	-1.08636300	-1.01975500
Cl	1.25118200	-0.04705100	1.39865200

Sum of electronic and zero-point Energies= -1632.305356
Sum of electronic and thermal Energies= -1632.298095
Sum of electronic and thermal Enthalpies= -1632.297151
Sum of electronic and thermal Free Energies= -1632.338898

TS | (IM2 [TCFE–OH]$^{\bullet}$ → *via* 1,3-H-migration → TS)

0 2

C	-0.72576200	-0.52970900	0.20642700
C	0.66724100	0.10402300	0.26431800
F	-0.73184400	-1.73659900	-0.38960400
Cl	-2.05067400	0.41035800	-0.48765800
O	-0.76972500	-0.62412500	1.56893000
H	0.46290600	-0.13645100	1.52053500
Cl	0.81217400	1.81129600	0.03334000
Cl	1.98159400	-0.85030300	-0.33333000

Sum of electronic and zero-point Energies= -1632.296775
Sum of electronic and thermal Energies= -1632.289840
Sum of electronic and thermal Enthalpies= -1632.288895
Sum of electronic and thermal Free Energies= -1632.330427

TS | (IM2 [TCFE–OH]$^{\bullet}$ → *via* 1,3-HCl-loss with cyclization → TS)

0 2

C	-0.44244200	-0.79827000	0.10932300
C	0.66468200	0.06899500	-0.25586200
F	-0.22976800	-2.08384000	0.34158000
Cl	-2.05777100	-0.52054300	-0.43532300
O	0.00168500	-0.03694200	1.24877800
H	-0.34374600	0.94264900	1.17123500
Cl	-0.12081000	2.36116200	-0.01301900
Cl	2.24121300	-0.51808400	-0.33733100

Sum of electronic and zero-point Energies= -1632.256156
Sum of electronic and thermal Energies= -1632.248911
Sum of electronic and thermal Enthalpies= -1632.247967
Sum of electronic and thermal Free Energies= -1632.290137

TS | (IM2 [TCFE–OH]$^{\bullet}$ → *via* F-atom loss → TS)

0 2

C	0.66967900	-0.55322700	-0.22969100
C	-0.53652900	0.11027000	-0.12271900
F	0.01560300	-0.29443100	1.79630500
Cl	2.16252400	0.27360100	-0.22036500
O	0.68671400	-1.85689200	-0.40078300
Cl	-1.98932900	-0.76278700	-0.26865900
Cl	-0.64024700	1.80675600	-0.14545500
H	1.50683700	-2.23594800	-0.05986700

Sum of electronic and zero-point Energies= -1632.303118
Sum of electronic and thermal Energies= -1632.295509
Sum of electronic and thermal Enthalpies= -1632.294565
Sum of electronic and thermal Free Energies= -1632.336953

TS | (IM2 [TCFE–OH]$^{\bullet}$ → *via* Cl-atom loss → TS)

0 2

C	1.19003800	0.16978700	-0.33127300
C	-0.19901900	0.08348200	-0.25911800
F	1.79063200	1.28446400	-0.04791600
O	2.01918700	-0.82351700	-0.48759300
H	1.53721100	-1.66060900	-0.56334800
Cl	-0.90154100	-1.28193400	-1.07581000
Cl	-1.09427200	1.54894200	-0.33164300
Cl	-0.34256900	-0.55118700	1.90378700

Sum of electronic and zero-point Energies= -1632.340804
Sum of electronic and thermal Energies= -1632.333309
Sum of electronic and thermal Enthalpies= -1632.332364
Sum of electronic and thermal Free Energies= -1632.374878

TS | (IM2 [TCFE–OH]$^{\bullet}$ → *via* 1,2-HCl-loss → TS)

0 2

C	-0.05412900	0.60212400	0.43754600
C	0.50239100	-0.69703700	0.38198000
F	-0.86319900	0.86907100	1.42870900
Cl	0.55930600	1.94345100	-0.36828900
O	-0.18203500	-1.68891400	0.77488300
H	-1.17997500	-1.45527400	0.37859200
Cl	2.02616700	-0.95623200	-0.33104300
Cl	-2.13162100	-0.53342900	-0.73320900

Sum of electronic and zero-point Energies= -1632.334103
Sum of electronic and thermal Energies= -1632.326814
Sum of electronic and thermal Enthalpies= -1632.325870
Sum of electronic and thermal Free Energies= -1632.368385

TS | (IM6 [TCFE–OH]$^{\bullet}$ → *via* 1,2-Cl-migration → TS)

0 2

C	0.59237200	-0.19830700	0.54112200
C	-0.77316200	-0.05089800	0.54154100
F	1.27932700	0.38295600	1.49205900
Cl	0.47102200	1.73433500	-1.02366800
O	-1.33056600	0.72944300	1.44817400
H	-2.08968400	1.20023900	1.07870000
Cl	-1.76942400	-0.87427800	-0.57021100
Cl	1.43399000	-1.38871400	-0.32309800

Sum of electronic and zero-point Energies= -1632.335390
Sum of electronic and thermal Energies= -1632.327832
Sum of electronic and thermal Enthalpies= -1632.326888
Sum of electronic and thermal Free Energies= -1632.369398

TS | (IM6 [TCFE–OH]$^{\bullet}$ → *via* 1,3-H-migration → TS)

0 2

C	-0.79019600	-0.62036800	0.22324500
C	0.55705700	0.09916400	0.30067000
F	-0.75788100	-1.85994200	-0.24426700
Cl	-2.22272700	0.22684700	-0.23631700
O	0.54250200	-0.00557300	1.67610100
H	-0.61874500	-0.59123700	1.52075600
Cl	0.59672300	1.78215100	-0.25195400
Cl	1.89062100	-0.80296800	-0.44553200

Sum of electronic and zero-point Energies= -1632.285721
Sum of electronic and thermal Energies= -1632.278682
Sum of electronic and thermal Enthalpies= -1632.277738
Sum of electronic and thermal Free Energies= -1632.319567

TS | (IM6 [TCFE–OH]$^{\bullet}$ → *via* Z-Cl-atom loss → TS)

0 2

C	-0.75610700	-0.13296000	0.51046200
C	0.53041300	0.34717600	0.55716200
F	-1.09713200	-1.09614700	1.32200600
Cl	-1.98798800	0.42858300	-0.49060000
O	1.36528200	-0.07914800	1.50054500
H	1.87951100	-0.82671900	1.15472100
Cl	0.91647000	-1.57655500	-1.02858700
Cl	0.97896400	1.73855600	-0.33157100

Sum of electronic and zero-point Energies= -1632.336329
Sum of electronic and thermal Energies= -1632.328524
Sum of electronic and thermal Enthalpies= -1632.327580
Sum of electronic and thermal Free Energies= -1632.371022

TS | (IM6 [TCFE–OH]$^{\bullet}$ → *via E*-Cl-atom loss → TS)

0 2

C	0.55748100	-0.58091000	-0.28209800
C	-0.54768100	-0.33129800	0.49079100
O	-0.45169900	-0.01420000	1.77586300
H	-0.27066300	0.93754800	1.85270300
Cl	-0.04515700	2.01845200	-0.39485100
Cl	2.14082300	-0.52203900	0.29924700
F	0.43229100	-0.96736900	-1.52077800
Cl	-2.09950000	-0.71078900	-0.11761700

Sum of electronic and zero-point Energies= -1632.336870
Sum of electronic and thermal Energies= -1632.329070
Sum of electronic and thermal Enthalpies= -1632.328125
Sum of electronic and thermal Free Energies= -1632.371492

C(O)Cl–$^{\bullet}$CClF | (IM6 [TCFE–OH]$^{\bullet}$ → *via* 1,2-HCl-loss → product)

0 2

C	-0.68875900	0.41430700	-0.00016500
C	0.74247500	0.59614300	-0.00034000
F	-1.41593000	1.50049600	0.00018300
Cl	-1.54422500	-1.03355500	-0.00018600
O	1.26197800	1.67006000	0.00028100
Cl	1.68100400	-0.90336500	0.00013600

Sum of electronic and zero-point Energies= -1171.575305
Sum of electronic and thermal Energies= -1171.569303
Sum of electronic and thermal Enthalpies= -1171.568359
Sum of electronic and thermal Free Energies= -1171.607266

$^{\bullet}$C(OH)Cl–CCl$_2$F | (IM6 [TCFE–OH]$^{\bullet}$ → *via* 1,2-Cl-migration → product)

0 2

C	0.57551900	-0.14308500	-0.29039900
C	-0.89988200	-0.20453000	-0.54840000
F	1.20108900	-0.81265300	-1.27180100
Cl	1.00891800	-0.94293900	1.25851000
O	-1.30682500	-1.43297800	-0.88414300
H	-2.26234400	-1.44973400	-1.00890600
Cl	-1.93579500	0.72629500	0.47552800
Cl	1.15354300	1.52918100	-0.28927000

Sum of electronic and zero-point Energies= -1632.356582
Sum of electronic and thermal Energies= -1632.348963
Sum of electronic and thermal Enthalpies= -1632.348019
Sum of electronic and thermal Free Energies= -1632.390688

C(•O)Cl_2–CHClF | (IM6 [TCFE–OH]• → *via* 1,3-H-migration → product)

0 2

C	-0.85948700	0.04376400	0.73059500
C	0.60486000	-0.18984900	0.29752600
F	-1.37102100	-1.15769800	1.08482400
Cl	-1.85639100	0.76831200	-0.52792400
O	1.32794700	-0.65685800	1.32271300
H	-0.85670200	0.70316900	1.59733300
Cl	1.39619900	1.39712800	0.01281900
Cl	0.70137300	-1.23323500	-1.13849400

Sum of electronic and zero-point Energies= -1632.333562
Sum of electronic and thermal Energies= -1632.326272
Sum of electronic and thermal Enthalpies= -1632.325328
Sum of electronic and thermal Free Energies= -1632.367310

(*Z*)-C(OH)Cl=CClF | ([TCFE–OH]• → *via* Cl-atom loss → product)

0 1

C	-0.65021700	0.43905000	0.01600700
C	0.67933100	0.42246900	-0.00291600
F	-1.29951700	1.59537900	0.02926600
Cl	-1.67650700	-0.92478700	-0.00920900
O	1.38108600	1.56643000	-0.10535300
H	2.09862300	1.57014000	0.53859000
Cl	1.58084000	-1.05339600	0.00699100

Sum of electronic and zero-point Energies= -1172.182308
Sum of electronic and thermal Energies= -1172.176029
Sum of electronic and thermal Enthalpies= -1172.175085
Sum of electronic and thermal Free Energies= -1172.213452

(*E*)-C(OH)Cl=CClF | ([TCFE–OH]• → *via* Cl-atom loss → product)

0 1

C	-0.54207400	-0.37173800	0.00623100
C	0.53018700	0.41141600	-0.00418200
O	0.44110700	1.74892000	-0.10143700
H	1.03005800	2.16367400	0.53926300
Cl	2.11910200	-0.27825700	0.00911000
Cl	-2.14765600	0.21002600	0.01538500
F	-0.44468600	-1.69257600	-0.01738500

Sum of electronic and zero-point Energies= -1172.183645
Sum of electronic and thermal Energies= -1172.177379
Sum of electronic and thermal Enthalpies= -1172.176435
Sum of electronic and thermal Free Energies= -1172.214784

Table S2. The expectation value of the $<S^2>$ operator at the M06-2X/6-311++G(d,p) level.

species / Quantum model	pre-RC1 (0,2)	pre-RC2 (0,2)	IM2 (0,2)	IM6 (0,2)	TS1 (0,2)	TS6 (0,2)
M06-2X/6-311++G(d,p)	0.7540	0.7546	0.7554	0.7547	0.7696	0.7749

Table S3. The temperature-dependent rates, Eckart tunneling corrections, and fitted Arrhenius two-parameters [$k=A.\exp(-E_a/RT)$] were computed using TST. (P = bar)

Parameter / Pathway	$T(K)$ ± 20%	$\kappa(T)$	k (s^{-1})	A (s^{-1})	E_a (kJ/mol)
TCFE+OH$^\bullet$ → **TS1** [TCFE…OH]$^\bullet$ → **IM2** [TCFE–OH]$^\bullet$ → *via* 1,2-HF-loss: → $^\bullet CCl_2$–C(O)Cl + HF					
	250	6.7	2.98E-16	2.97E+12	134.01
	270	5.15	3.59E-14	4.02E+12	134.65
	290	4.17	2.28E-12	5.17E+12	135.22
	298	3.87	1.03E-11	5.65E+12	135.44
	310	3.51	8.59E-11	6.39E+12	135.74
	330	3.04	2.11E-09	7.65E+12	136.21
	350	2.70	3.62E-08	8.92E+12	136.64
	370	2.44	4.61E-07	1.02E+13	137.02
	390	2.24	4.55E-06	1.14E+13	137.38
	410	2.08	3.61E-05	1.26E+13	137.70
	430	1.95	2.37E-04	1.38E+13	138.00
	450	1.84	1.32E-03	1.49E+13	138.28
TCFE+OH$^\bullet$ → **TS1** [TCFE…OH]$^\bullet$ → **IM2** [TCFE–OH]$^\bullet$ → *via* 1,2-F-migration: → CCl_2F–$^\bullet$C(OH)Cl					
	250	1.07	2.94E-22	7.56E+12	164.70
	270	1.06	1.05E-19	8.28E+12	164.89
	290	1.05	1.66E-17	8.95E+12	165.06
	298	1.05	1.05E-16	9.20E+12	165.13
	310	1.04	1.38E-15	9.56E+12	165.23
	330	1.04	6.75E-14	1.01E+13	165.38
	350	1.03	2.12E-12	1.07E+13	165.52
	370	1.03	4.59E-11	1.11E+13	165.65
	390	1.03	7.28E-10	1.15E+13	165.76
	410	1.02	8.82E-09	1.19E+13	165.85
	430	1.02	8.48E-08	1.22E+13	165.94
	450	1.02	6.68E-07	1.25E+13	166.03
TCFE+OH$^\bullet$ → **TS1** [TCFE…OH]$^\bullet$ → **IM2** [TCFE–OH]$^\bullet$ → *via* 1,3-HCl-loss with cyclization: → $^\bullet$CCl(O)CClF + HCl					
	250	1.08	1.27E-46	6.65E+12	281.04
	270	1.07	2.85E-42	6.90E+12	281.12
	290	1.06	1.61E-38	7.11E+12	281.19
	298	1.06	3.68E-37	7.19E+12	281.21
	310	1.05	2.98E-35	7.30E+12	281.25
	330	1.05	2.22E-32	7.46E+12	281.31
	350	1.04	7.79E-30	7.60E+12	281.36
	370	1.04	1.45E-27	7.72E+12	281.40
	390	1.03	1.58E-25	7.84E+12	281.45
	410	1.03	1.09E-23	7.92E+12	281.49
	430	1.03	5.08E-22	8.03E+12	281.53
	450	1.03	1.68E-20	8.13E+12	281.58

Continued Table S3:

Pathway \ Parameter	$T(K) \pm 20\%$	$\kappa(T)$	k (s^{-1})	A (s^{-1})	E_a (kJ/mol)
TCFE+OH$^\bullet$ → **TS1** [TCFE…OH]$^\bullet$ → **IM2** [TCFE–OH]$^\bullet$ → *via* F-atom loss: → CCl_2=C(OH)Cl + F$^\bullet$					
	250	1.07	2.94E-22	7.56E+12	164.70
	270	1.06	1.05E-19	8.28E+12	164.89
	290	1.05	1.66E-17	8.95E+12	165.06
	298	1.05	1.05E-16	9.20E+12	165.13
	310	1.04	1.38E-15	9.56E+12	165.23
	330	1.04	6.75E-14	1.01E+13	165.38
	350	1.03	2.12E-12	1.07E+13	165.52
	370	1.03	4.59E-11	1.11E+13	165.65
	390	1.03	7.28E-10	1.15E+13	165.76
	410	1.02	8.82E-09	1.19E+13	165.85
	430	1.02	8.48E-08	1.22E+13	165.94
	450	1.02	6.68E-07	1.25E+13	166.03
TCFE+OH$^\bullet$ → **TS1** [TCFE…OH]$^\bullet$ → **IM2** [TCFE–OH]$^\bullet$ → *via* 1,3-H-migration: → $CHCl_2$–C(O$^\bullet$)ClF					
	250	16.20	6.47E-23	6.63E+11	162.78
	270	11.66	2.16E-20	7.71E+11	163.10
	290	8.86	3.26E-18	8.82E+11	163.40
	298	8.05	2.02E-17	9.27E+11	163.52
	310	7.04	2.60E-16	9.95E+11	163.70
	330	5.79	1.23E-14	1.11E+12	163.98
	350	4.90	3.76E-13	1.22E+12	164.25
	370	4.24	7.97E-12	1.34E+12	164.51
	390	3.74	1.24E-10	1.45E+12	164.76
	410	3.35	1.49E-09	1.56E+12	165.00
	430	3.04	1.42E-08	1.67E+12	165.23
	450	2.80	1.11E-07	1.78E+12	165.46
TCFE+OH$^\bullet$ → **TS1** [TCFE…OH]$^\bullet$ → **IM2** [TCFE–OH]$^\bullet$ → *via* 1,2-HCl-loss: → $^\bullet CCl_2$–C(O)F + HCl					
	250	1.43	3.25E-01	1.04E+13	64.64
	270	1.36	3.27E+00	1.13E+13	64.81
	290	1.31	2.40E+01	1.20E+13	64.95
	298	1.29	4.95E+01	1.22E+13	64.99
	310	1.26	1.37E+02	1.26E+13	65.06
	330	1.23	6.33E+02	1.30E+13	65.15
	350	1.20	2.46E+03	1.34E+13	65.23
	370	1.18	8.28E+03	1.37E+13	65.30
	390	1.16	2.46E+04	1.39E+13	65.36
	410	1.15	6.58E+04	1.42E+13	65.40
	430	1.13	1.61E+05	1.43E+13	65.45
	450	1.12	3.63E+05	1.45E+13	65.48

Continued Table S3:

Pathway \ Parameter	$T(K) \pm 20\%$	$\kappa(T)$	k (s^{-1})	A (s^{-1})	E_a (kJ/mol)
TCFE+$OH^{\bullet}$ → **TS1** [TCFE…OH]$^{\bullet}$ → **IM2** [TCFE–OH]$^{\bullet}$ → *via* 1,2-Cl-migration: → CCl_3–$^{\bullet}$C(OH)F					
	250	1.31	2.57E-21	3.36E+12	158.50
	270	1.26	7.32E-19	3.63E+12	158.67
	290	1.22	9.61E-17	3.89E+12	158.83
	298	1.21	5.64E-16	3.99E+12	158.89
	310	1.19	6.76E-15	4.12E+12	158.97
	330	1.16	2.85E-13	4.34E+12	159.10
	350	1.14	7.84E-12	4.53E+12	159.22
	370	1.13	1.51E-10	4.70E+12	159.33
	390	1.11	2.16E-09	4.86E+12	159.43
	410	1.10	2.37E-08	4.99E+12	159.52
	430	109	2.10E-07	5.12E+12	159.60
	450	1.08	1.53E-06	5.23E+12	159.68
TCFE+$OH^{\bullet}$ → **TS1** [TCFE…OH]$^{\bullet}$ → **IM2** [TCFE–OH]$^{\bullet}$ → *via* Cl-atom loss: → CCl_2=C(OH)F + $Cl^{\bullet}$					
	250	1.03	4.24E-02	9.53E+12	68.69
	270	1.03	4.92E-01	1.01E+13	68.81
	290	1.02	4.08E+00	1.06E+13	68.92
	298	1.02	8.80E+00	1.07E+13	68.96
	310	1.02	2.59E+01	1.10E+13	69.01
	330	1.02	1.31E+02	1.13E+13	69.08
	350	1.01	5.54E+02	1.15E+13	69.14
	370	1.01	2.00E+03	1.17E+13	69.19
	390	1.01	6.34E+03	1.18E+13	69.21
	410	1.01	1.80E+04	1.19E+13	69.24
	430	1.01	4.62E+04	1.19E+13	69.25
	450	1.00	1.09E+05	1.20E+13	69.26

Table S4. Energetic and thermodynamic parameters for the secondary pathways of the energized adducts **IM2** and **IM6** at the M06-2X level of theory (P =1 bar, T =298 K) (All the energies are in units of kcal mol^{-1}, except ΔS° in units of cal mol^{-1} K^{-1}).

Species \ Parameters	ΔE_{0K}	$\Delta H°_{298K}$	$\Delta G°_{298K}$	$\Delta E_{0K}^{\dagger}$	$\Delta H°_{298K}^{\dagger}$	$\Delta G°_{298K}^{\dagger}$	$\Delta S°_{298K}^{\dagger}$
Fate of reaction of energized adducts IM2							
IM2 [TCFE-OH]$^{\bullet}$ + O_2 → pre-reactive IM3b [TCFE-OH…O_2]$^{\bullet}$	–2.901	–2.966	5.664				
IM2 [TCFE-OH]$^{\bullet}$ + O_2 → TS2b → IM3b [TCFE-OH–O_2]$^{\bullet}$	–20.354	–21.309	–8.932	–0.462	–1.016	9.984	–36.892
IM3b [TCFE-OH–O_2]$^{\bullet}$ + NO → pre-reactive IM4b [TCFE-OH-OO…NO]	–23.639	–24.463	–12.504				
IM3b [TCFE-OH–O_2]$^{\bullet}$ + NO → TS3 → IM4 [TCFE-OH–O]$^{\bullet}$ + NO_2	–14.375	–14.654	–15.988	–1.861	–2.363	8.308	–35.79
IM3b [TCFE-OH–O_2]$^{\bullet}$ + HO_2 → TS3a → IM4a [TCFE-OH–O_2H] + O_2	–43.215	–43.229	–41.558				
IM4 [TCFE-OH–O]$^{\bullet}$ → TS4a → $^{\bullet}$Cl + C(O)Cl–C(OH)ClF	–8.434	–7.764	–17.043	4.337	4.292	4.208	0.282
IM4 [TCFE-OH–O]$^{\bullet}$ → TS4b → $COCl_2$ + IM5 [$^{\bullet}$C(OH)ClF]	–4.617	–4.184	–17.548	0.676	0.602	0.694	-0.31
IM5 [$^{\bullet}$C(OH)ClF] + O_2 → pre-reactive IM6b [$^{\bullet}$C(OH)ClF…O_2]$^{\bullet}$	–35.367	–35.493	–26.709				
IM5 [$^{\bullet}$C(OH)ClF] + O_2 → TS5 → HO_2 + CClFO	–29.358	–29.462	–29.998	–25.488	–26.862	–14.486	–41.509
Fate of reaction of energized adducts IM6							
IM6 [TCFE-OH]$^{\bullet}$ + O_2 → pre-reactive IM7b [TCFE-OH…O_2]$^{\bullet}$	–26.166	–27.137	–14.898				
IM6 [TCFE-OH]$^{\bullet}$ + O_2 → TS7b → IM7b [TCFE-OH–O_2]$^{\bullet}$	–27.549	–28.546	–16.254	–0.905	–1.372	9.181	13.528
IM7b [TCFE-OH–O_2]$^{\bullet}$ + NO → pre-reactive IM8b [TCFE-OH-OO…NO]	–23.084	–23.874	–12.061				
IM7b [TCFE-OH–O_2]$^{\bullet}$ + NO → TS8 → IM8 [TCFE-OH–O]$^{\bullet}$ + NO_2	–15.358	–15.618	–17.007	2.220	0.618	13.065	–39.761
IM7b [TCFE-OH–O_2]$^{\bullet}$ + HO_2 → TS8a → IM8a [TCFE-OH–O_2H] + O_2	–44.115	–44.105	–42.447				
IM8 [TCFE-OH–O]$^{\bullet}$ → TS9a → $^{\bullet}$Cl + C(OH)Cl_2–C(O)F	–7.176	–6.476	–15.673	–0.109	–0.611	9.874	–35.163
IM8 [TCFE-OH–O]$^{\bullet}$ → TS9c → $^{\bullet}$F + C(OH)Cl_2–C(O)Cl	28.026	28.943	19.507	35.774	35.909	35.537	1.249
IM8 [TCFE-OH–O]$^{\bullet}$ → TS9b → COClF + IM9 [$^{\bullet}$C(OH)Cl_2]	–7.472	–7.068	–20.718	6.786	6.696	6.855	–0.534
IM9 [$^{\bullet}$C(OH)Cl_2] + O_2 → pre-reactive IM10b [$^{\bullet}$C(OH)Cl_2…O_2]$^{\bullet}$	–32.320	–32.338	–23.964				
IM9 [$^{\bullet}$C(OH)Cl_2] + O_2 → TS10 → HO_2 + $COCl_2$	–26.421	–26.492	–26.697	–20.918	–22.180	–9.930	–41.084

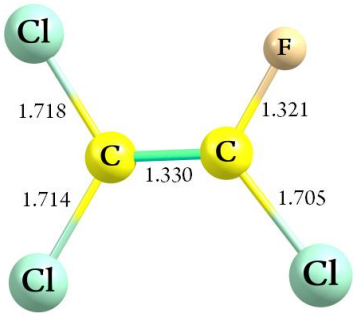

TCFE

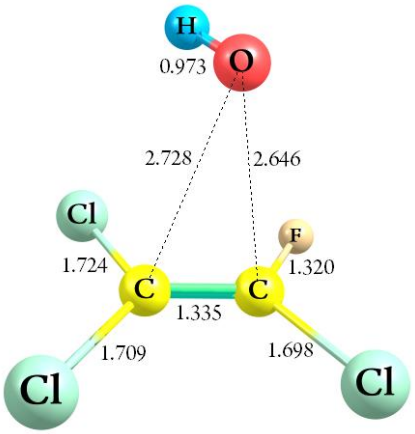

pre-RC1

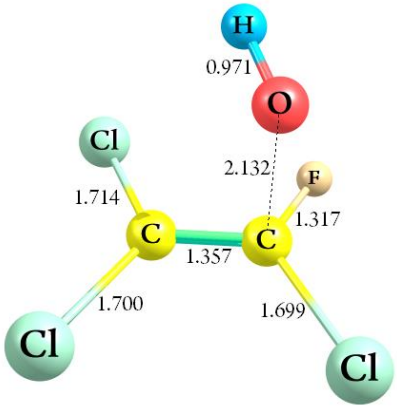

TS1 (denoted as TS1)

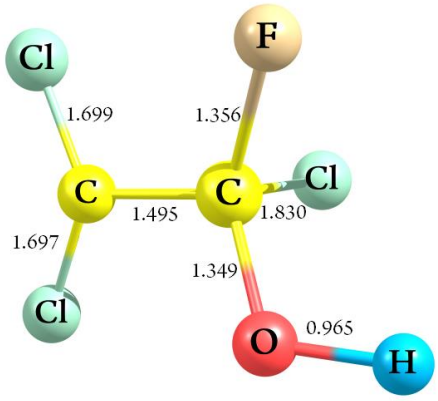

P1 (denoted IM2)

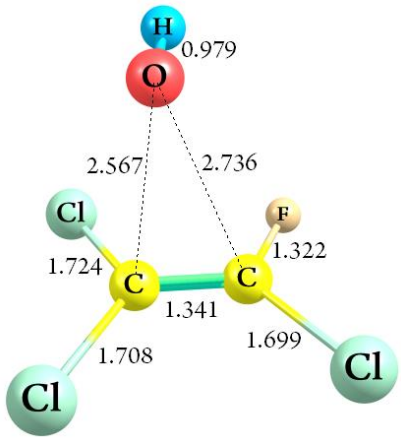

pre-RC2

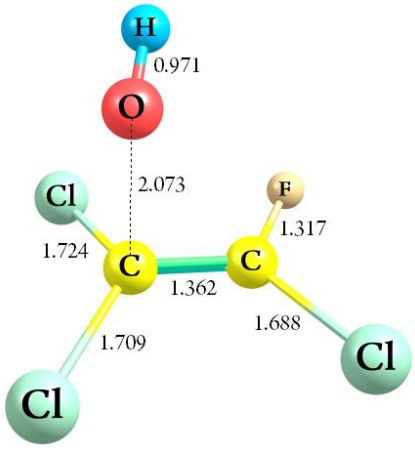

TS2 (denoted TS6)

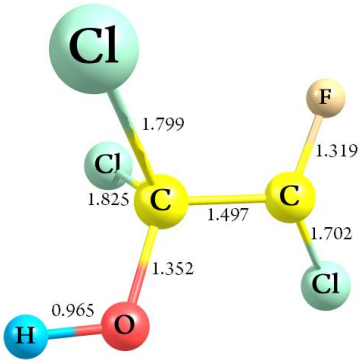

P2 (denoted IM6)

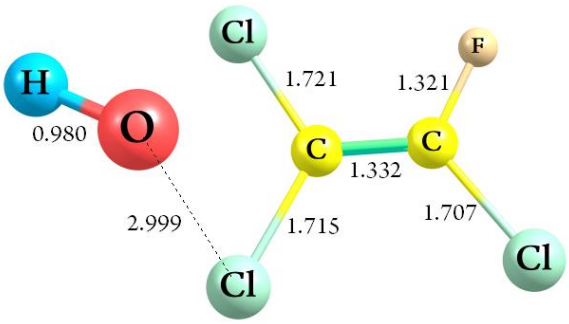

pre-RC3

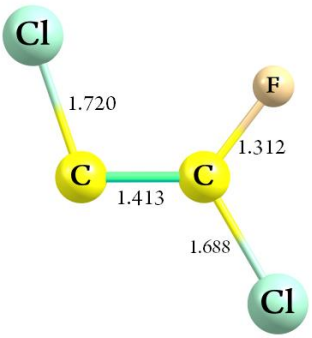

P3

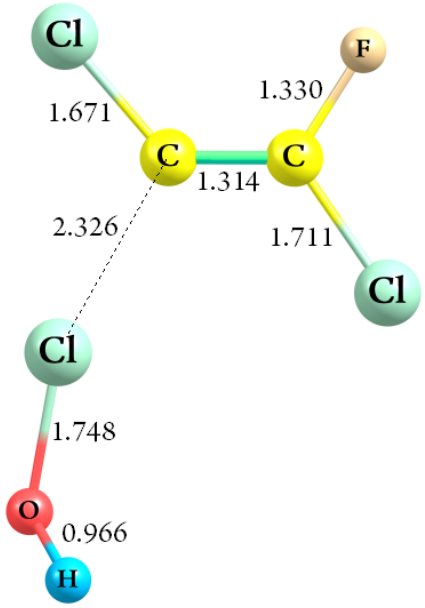

TS3 (denoted TS11)

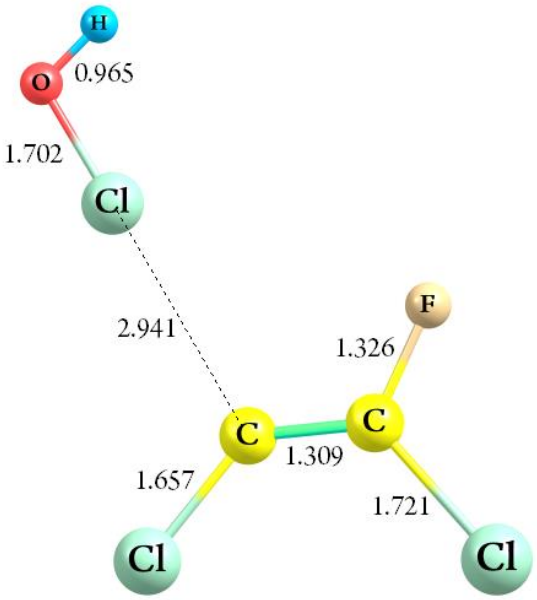

TS4 (denoted TS12)

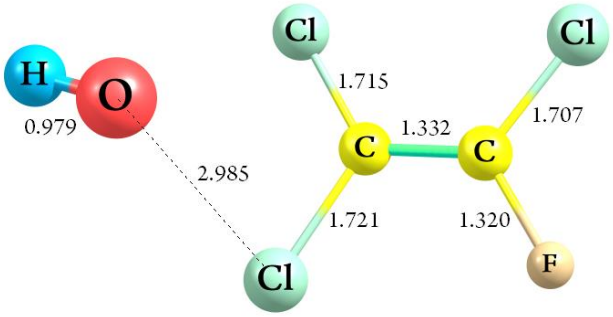

pre-RC4

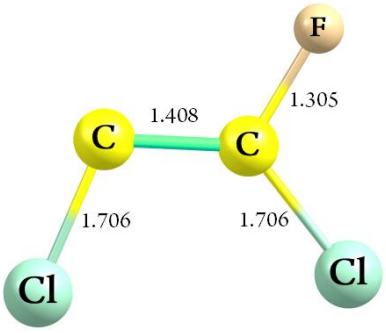

P4

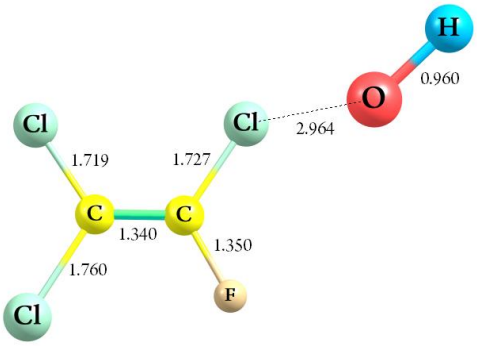

pre-RC5

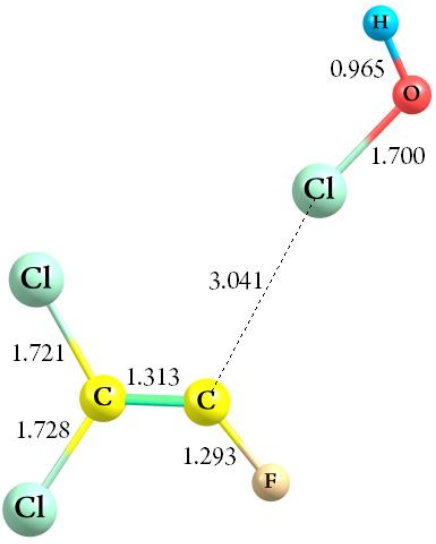

TS5 (denoted TS13)

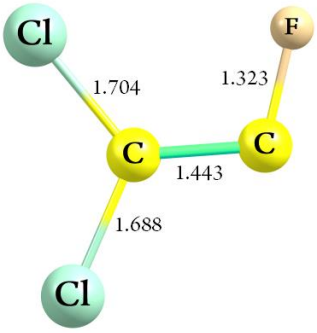

P5

Fig. S1. Optimized structures of all stationary points along with the TCFE+$OH^{\bullet}$+O_2 reaction system, at the M06-2X/6-311++G(d,p) level of theory. Bond lengths are given in angstroms (Å). (see also Table S1 in the SI).

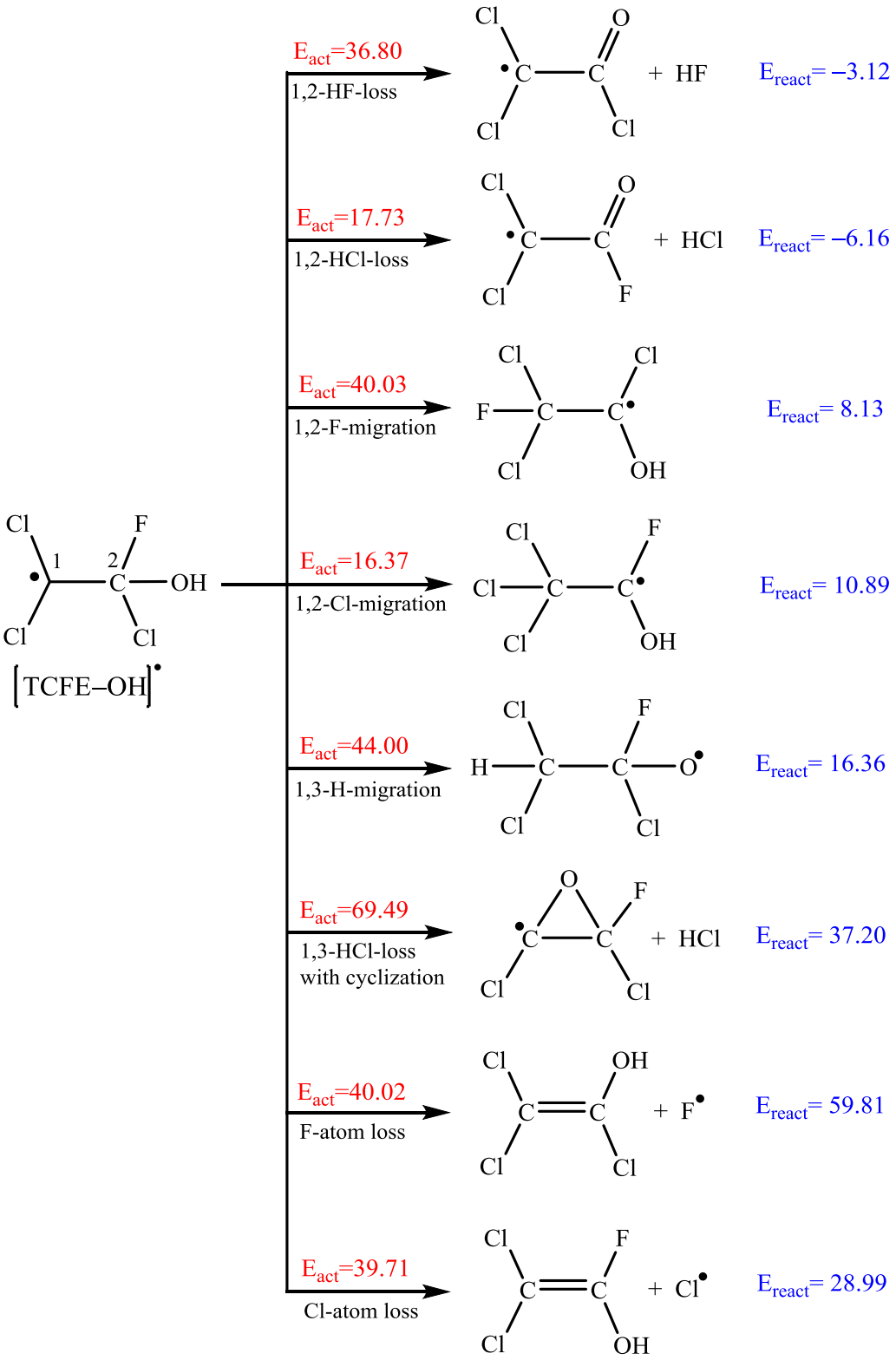

Fig. S2. All pathways are considered the most stable adduct at the M06-2X method.

(All energy barriers and reaction relative energies in kcal mol^{-1})

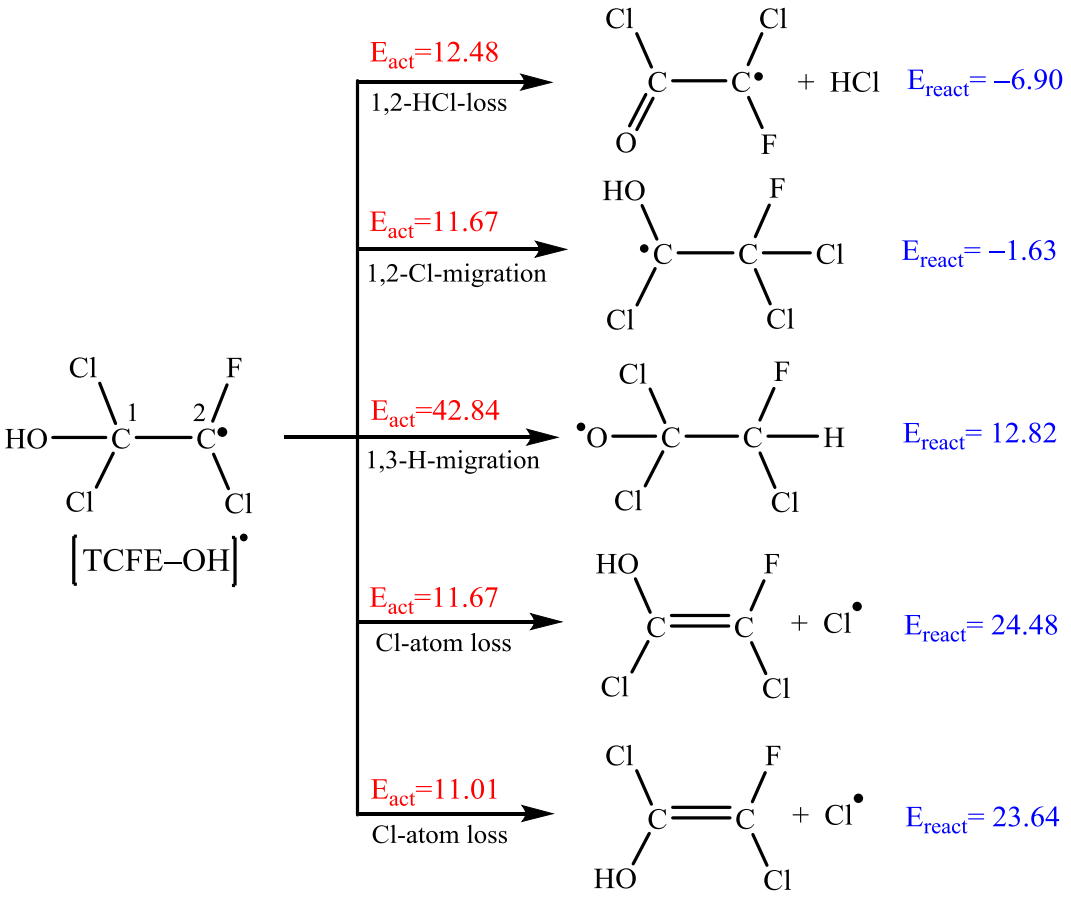

Fig. S3. All pathways are considered the minor adduct at the M06-2X method.

(All energy barriers and reaction relative energies in kcal mol^{-1})